UNIVERSIDADE D
COIMBRA

Leonardo Filipe Kleman Santos

Synthesis of new BODIPYs for Photodynamic Therapy

Dissertação no âmbito do Mestrado em Química Avançada orientada pelo Professor Doutor Abílio José Nascimento Fraga Sobral e apresentada ao Departamento de Química da Faculdade de Ciências e Tecnologia da Universidade de Coimbra

Fevereiro de 2023

UNIVERSIDADE D
COIMBRA

Leonardo Filipe Kleman Santos

Synthesis of new BODIPYs for photodynamic therapy

Dissertação no âmbito do Mestrado em Química Avançada orientada pelo Professor Doutor Abílio José Fraga Nascimento Sobral e apresentada ao Departamento de Química da Faculdade de Ciências e Tecnologia da Universidade de Coimbra

Fevereiro de 2023

Agradecimentos

Em primeiro lugar, começo por agradecer ao Professor Doutor Abílio Sobral do Departamento de Química, a oportunidade dada para a realização da tese de mestrado no seu grupo de investigação, bem como a ajuda constante e sempre presente.

Também não posso deixar de mencionar que o Professor despoletou o meu interesse pela química orgânica, e sempre me incentivou na continuação dos estudos na área.

Agradeço à Professora Doutora Filomena Botelho e Doutora Mafalda Laranjo pela oportunidade de trabalhar no Instituto de Biofísica, permitindo-me ganhar conhecimentos e experiência na área biológica através dos estudos realizados nas culturas celulares.

Agradeço igualmente a todos os elementos do grupo de investigação, especialmente à Juliana Araújo e à Chrislaura Carmo pela ajuda e apoio ao longo destes anos, proporcionando um ótimo ambiente de trabalho.

Outro agradecimento vai para o Professor Joaquim Marques Santos da Escola Secundária Jacome Ratton de Tomar, que me incentivou a perseguir o ramo fascinante da Química e continuar neste percurso incrível que me forma como químico. Um excelente professor que através da sua partilha de conhecimento nas aulas de Físico-Química, despertou o meu interesse na área.

Agradeço ao Diogo Barradas do Laboratório de Termodinâmica do Departamento de Química, a ajuda e disponibilidade constante para estudos de Infravermelho, também como a Professora Ermelinda Eusébio pela disponibilidade e marcação do equipamento.

Agradeço também à Ana Clara e João Ferreira do Laboratório de Fotoquímica do Departamento de Química pelo acompanhamento e ajuda nos estudos fotoquímicos e ao Professor Doutor Sérgio Seixas de Melo pela disponibilidade e marcação de equipamentos.

Agradeço igualmente ao Dr. Pedro Cruz pelos espetros de RMN, pela disponibilidade e ajuda.

Agradeço a todos os meus colegas principalmente ao Diogo Barradas, Iuri Tavares, João Ferreira, Zoé Arnaut, Alexandre Felgueiras, Vitaliy Masliy, Carolina Amaral, Maria Sousa, José Morgado e João Coelho pela amizade e bons tempos passados, e com principal atenção à Ana Fontes, uma pessoa incrível e espetacular que esteve sempre em todos os momentos e, que foi e será uma das pessoas mais

fantásticas e com mais impacto na minha vida, um grande obrigado. Por fim, agradeço à minha família pelo apoio em todos os momentos, onde me ajudaram e estiveram sempre lá presentes por mim.

Index

Abbreviations v
Structures vii
Table of Figures ix
Table of Schemes xiii
Abstract xv
Resumo xvii
Introduction 1
1.1 Medicinal Chemistry 1
1.2 Photodynamic Therapy 2
1.3 BODIPY Molecules 6
Experimental 9
2.1 Reagents and Solvents 9
2.2 Instrumentation 9
2.2.1 Mass spectrometry 9
2.2.2 Nuclear magnetic resonance spectroscopy 9
2.2.3 UV-vis spectroscopy 9
2.2.4 Spectrofluorometer 10
2.3 Synthetic procedures 10
2.3.1 Procedures for the synthesis of BODIPY 1 using DCM 10
2.3.2 General procedures for the synthesis of BODIPY 1,3 and 4 using THF 11
2.3.3 Bromination of BODIPY 1 13
2.3.4 General procedures for the synthesis of BODIPYs 6 and 7 13
2.4 *In Vitro* studies 15
2.4.1 Photodynamic Therapy 15
2.4.2 MTT Studies 15
Results and Discussion 17
3.1 Synthesis of Aromatic BODIPYs 17
3.1.1 Synthesis of BODIPY dimer (BODIPY 1) using DCM 17
3.1.2 Synthesis of BODIPY dimer (BODIPY 1) using THF 27
3.1.3 Synthesis of Meso-Phenyl-BODIPY (BODIPY 3) 33
3.1.4 Synthesis of BODIPY trimer (BODIPY 4) 37

3.1.5 Preliminary studies in the bromination of the BODIPY dimer 42
3.2 Synthesis of Aliphatic BODIPYs 45
3.2.1 Synthesis of Meso-Iso-Propyl-BODIPY (BODIPY 6) 45
3.2.2 Synthesis of Meso-Methyl-BODIPY (BODIPY 7) 50
3.3 Biological Studies 52
3.3.1 Metabolic activity 53
Conclusion 57
Future perspectives 58
References 59

Abbreviations

^{1}H-NMR	Protonic Nuclear Magnetic Resonance
^{11}B-NMR	Boron-11 Nuclear Magnetic Resonance
^{13}C-NMR	Carbon-13 Nuclear Magnetic Resonance
^{19}F-NMR	Fluorine-19 Nuclear Magnetic Resonance
ACN	Acetonitrile
BODIPY	4,4-difluoro-4-bora-3a, 4a-diaza-s-indacene
$CDCl_3$	Deuterated chloroform
d	Duplet
DCM	Dichloromethane
DDQ	2,3-dichloro-5,6-dicyano-p-benzoquinone
DMF	Dimethylformamide
DMSO	Dimethylsulfoxide
m	Multiplet
MTT	3-(4,5-dimethylthiazol-2-yl)-2,5-diphenyltetrazolium bromide)
NADH	Nicotinamide adenine dinucleotide
NADPH	Nicotinamide adenine dinucleotide phosphate
NIR	near infrared
PDT	Photodynamic therapy
ppm	Parts per million
q	Quartet
s	Singlet
t	Triplet
TFA	Trifluoroacetic acid
THF	Tetrahydrofuran
TLC	Thin layer chromatography
TMS	Tetramethylsilane
UV/Vis	UV–visible spectroscopy

Structures

BODIPY dimer
(BODIPY 1)

10,10'-(1,4-phenylene)bis(2,8-diethyl-5,5-difluoro-1,3,7,9-tetramethyl-5H-dipyrrolo[1,2-c:2',1'-f][1,3,2]diazaborinin-4-ium-5-uide)

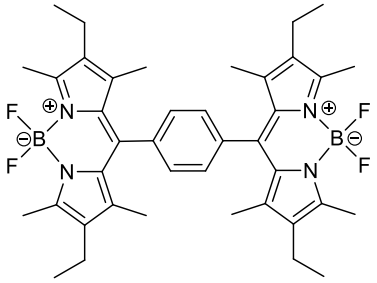

Core
(BODIPY 2)

2,8-diethyl-5,5-difluoro-1,3,7,9-tetramethyl-5H-dipyrrolo[1,2-c:2',1'-f][1,3,2]diazaborinin-4-ium-5-uide

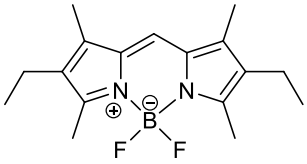

Meso-Phenyl-BODIPY
(BODIPY 3)

2,8-diethyl-5,5-difluoro-1,3,7,9-tetramethyl-10-phenyl-5H-dipyrrolo[1,2-c:2',1'-f] [1,3,2]diazaborinin-4-ium-5-uide

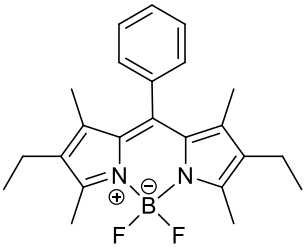

BODIPY trimer
(BODIPY 4)

10,10',10''-(benzene-1,3,5-triyl)tris(2,8-diethyl-5,5-difluoro-1,3,7,9-tetramethyl-5H-dipyrrolo[1,2-c:2',1'-f][1,3,2]diazaborinin-4-ium-5-uide)

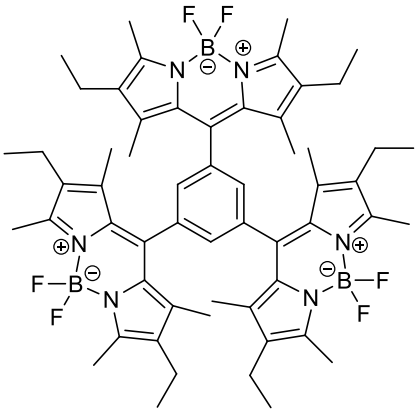

Meso-Bromo-Phenyl-BODIPY (BODIPY 5)	10-(4-bromophenyl)-2,8-diethyl-5,5-difluoro-1,3,7,9-tetramethyl-5H-dipyrrolo[1,2-c:2',1'-f][1,3,2]diazaborinin-4-ium-5-uide 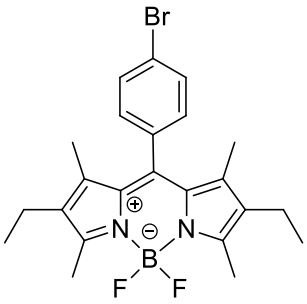
Meso-Iso-propyl-BODIPY (BODIPY 6)	2,8-diethyl-5,5-difluoro-10-isopropyl-1,3,7,9-tetramethyl-5H-dipyrrolo[1,2-c:2',1'-f] [1,3,2]diazaborinin-4-ium-5-uide 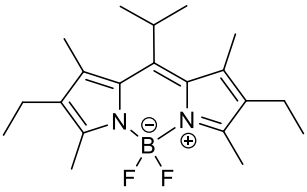
Meso-Methyl-BODIPY (BODIPY 7)	2,8-diethyl-5,5-difluoro-1,3,7,9,10-pentamethyl-5H-dipyrrolo[1,2-c:2',1'-f][1,3,2]diazaborinin-4-ium-5-uide 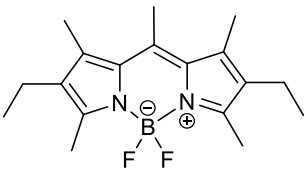

Table of Figures

Figure 1- Molecular structure of Atorvastatin, Fluticasone and Clopidogrel. 1
Figure 2- Structures of Infliximab, erythropoietin, and insulin glargine 1
Figure 3- Chemical structure of lithium carborate and cisplatin. 2
Figure 4- Photodynamic Therapy scheme (adapted from [30]). 4
Figure 5- Chart of the estimated number of new cases in 2020.[19] 5
Figure 6- 4,4-difluoro-4-bora-3a,4a-diaza-s-indacene. 7
Figure 7- Positions and nomenclature of BODIPYs molecules. 7
Figure 8- TLC and bidimensional TLC of the dimer and the core. 18
Figure 9 - ^{1}H NMR spectrum of BODIPY dimer. 19
Figure 10 - ^{1}H NMR spectrum of the core. 20
Figure 11- Mass spectrum of the BODIPY dimer. 21
Figure 12- Chemical structure of fragments representing the core and phenyl-BODIPY. 21
Figure 13 - Mass spectrum of the fragment 683.5 m/z. 22
Figure 14 - Mass spectrum of the BODIPY core. 22
Figure 15 - ESI Full MS^{2} Mass spectrum of the 304.2 ion. 23
Figure 16 - Infrared ATR spectrum of terephthaldehyde, BODIPY dimer and the core. 24
Figure 17- Absorption, emission, and excitation spectra of the dimer in toluene. 25
Figure 18- Absorption, emission, and excitation spectra of the dimer in ACN. 25
Figure 19- Absorption, emission, and excitation spectra of the dimer in DMSO. 26
Figure 20- Absorption, emission, and excitation spectra of the dimer in THF. 26
Figure 21- Quantum yield equation. 27
Figure 22- Chemical structure of Rhodamine 6G. 27
Figure 23- TLC of the dimer formed by THF, DCM and the mixture of both. 28
Figure 24- Normalized absorption spectra of the BODIPY dimer. 29
Figure 25- ^{1}H NMR of the BODIPY dimer synthesized in THF. 30
Figure 26- ^{13}C NMR of the BODIPY dimer synthetised in THF. 31
Figure 27- ^{19}F NMR of the BODIPY dimer synthesized in THF. 32
Figure 28- ^{11}B NMR of the BODIPY dimer synthesized in THF. 32
Figure 29 - ^{1}H NMR spectrum of Meso-Phenyl-BODIPY. 33
Figure 30 - (A) " ^{13}C NMR spectrum of Meso-Phenyl-BODIPY" ; (B) " ^{19}F NMR spectrum of Meso-Phenyl-BODIPY" and " ^{11}B NMR spectrum of Meso-Phenyl-BODIPY". 34

Figure 31 - Mass spectrum of Meso-Phenyl-BODIPY. 35
Figure 32 - MS^2 mass spectrum of the fragment 381.3 m /z. 35
Figure 33- Absorption spectrum (A) and ATR spectrum (B) of the Meso-Phenyl-BODIPY 36
Figure 34- Absorption, emission, and excitation spectra of Meso-Phenyl-BODIPY. 36
Figure 35- Absorption spectraof all 5 fractions formed in the BODIPY trimer reaction. 37
Figure 36- UV-vis spectrum of the F2 compound 38
Figure 37- Mass spectrum of the fraction F2. 39
Figure 38- MS^2 spectrum of the fraction F2. 40
Figure 39- ^1H NMR spectrum of fraction F2. 40
Figure 40- Full MS spectrum of the BODIPY trimer. 41
Figure 41- MS^2 of the BODIPY trimer. 41
Figure 42- ^1H NMR of the BODIPY trimer. 42
Figure 43 - Molecular structure of N-bromo succinimide and succinimide. 43
Figure 44- Absorption spectra of the bromination of the dimer. 44
Figure 45 - UV-vis spectrum of Phenyl-BODIPY, Bromo-Phenyl-BODIPY and the product of the bromination of Phenyl-BODIPY. 45
Figure 46- Normalised absorption spectrum of iso-propyl-BODIPY. 46
Figure 47 - ^1H NMR spectrum of Meso-Iso-Propyl-BODIPY. 47
Figure 48- (A) "^{13}C NMR spectrum of Meso-Iso-Propyl-BODIPY"; (B) "^{19}F NMR spectrum of Meso-Iso-Propyl-BODIPY" and (C) "^{11}B NMR spectrum of Meso-Iso-Propyl-BODIPY" 48
Figure 49- Mass spectrum of iso-propyl-BODIPY. 49
Figure 50- MS^2 of Meso-Iso-Propyl-BODIPY. 49
Figure 51- Absorption spectrum of Meso-Methyl-BODIPY. 50
Figure 52- ^1H NMR spectrum of Meso-Methyl-BODIPY. 51
Figure 53- MS spectrum of Meso-Methyl-BODIPY. 51
Figure 54- MS^2 of the Meso-Methyl-BODIPY. 52
Figure 55- (A) A549 cell line (B) H1299 cell line. 52
Figure 56 - Metabolic activity of BODIPY dimer and Meso-Phenyl BODIPY in the adenocarcinoma human alveolar basal epithelial cells, A549. Cells were incubated with BODIPYs and maintained in the dark or submitted to PDT with light exposure until 10J. The evaluation of the metabolic activity was carried out after 24 and 48 hours. Results are presented as the mean and standard deviation of, at least, three experiments. 53

Figure 57 - Metabolic activity of BODIPY dimer and Meso-Phenyl BODIPY in the human non-small cell lung carcinoma cell line, H1299. Cells were incubated with BODIPYs and maintained in the dark or submitted to PDT with light exposure until 10J. The evaluation of the metabolic activity was carried out after 24 and 48 hours. Results are presented as the mean and standard deviation of, at least, three experiments. 54

Table of Schemes

Scheme 1- Synthesis of a BODIPY from a pyrrole molecule and an aldehyde 17

Scheme 2- Synthesis of the BODIPY dimer 18

Scheme 3- Synthesis of the BODIPY dimer using THF 28

Scheme 4- Synthesis of Meso-Phenyl-BODIPY 33

Scheme 5- Synthesis of the BODIPY trimer 37

Scheme 6- Synthesis of Iso-Propyl-BODIPY 45

Scheme 7- Synthesis of Meso-Methyl-BODIPY 50

Abstract

Boron-dipyrromethene (BODIPYs) are an important group of compounds studied for application in various areas, in particular medicine, chemistry, and sometimes in physics.

These molecules are known to have small stokes Shift, narrow absorption bands, sharp emission bands, high fluorescence, quantum yields, and excellent chemical and photostability, which make them interesting to photodynamic therapy, cellular imaging, and drug delivery but also as organic photovoltaic materials.

This work aimed to synthesize and characterize new aromatic and aliphatic BODIPYs and, posteriorly, evaluate their biological activity in i*n vitro* studies, for photodynamic therapy.

The synthesis of BODIPYs involved the condensation of an alpha-free pyrrole and aldehydes in the presence of an acid, forming a dipyrromethane intermediate which was oxidized to the corresponding dipyromethene. After, dipyrromethene was complexed with boron trifluoride in the presence of a base. The change of solvent, from dichloromethane to tetrahydrofuran, in the procedure was also studied and giving better yields. The study of the possibility of conducting photo-oxidation of the dipyrromethane instead of using the usual chemical oxidation with DDQ, was also studied.

All BODIPYs synthesized were characterized by NMR, absorption and emission spectroscopy, and mass spectrometry. BODIPY dimer and Meso-phenyl BODIPY were studied as potential photosensitizers in PDT in two lung cancer cell lines, H1299 and A549. Cytotoxicity and phototoxicity using MTT assay were evaluated for 24 and 48h. BODIPY dimer did not show cytotoxicity or phototoxicity for all conditions. However, Meso-Phenyl BODIPY showed cytotoxic for higher concentrations and phototoxicity for A549 cell line.

In summary, the current study provided insights into the synthesis of BODIPY with considerable advances in terms of process optimization, with supported results of primary laboratory trial tests on lung cancer cells. Based on the results, BODIPY dimer can be a good candidate for diagnosis, once it is not toxic and BODIPY Meso-Phenyl a candidate for PDT.

Keywords: BODIPY; organic synthesis; photo-oxidation; lung cancer, photodynamic therapy.

Resumo

Moléculas de boro-dipirrometeno são um importante grupo de compostos estudados para aplicação em diversas áreas, como na medicina, na química e, por vezes, na física.

Estas moléculas são conhecidas por terem pequenos desvios de Stokes, bandas de absorção e bandas de emissão fortes, elevada fluorescência, rendimentos quânticos e foto-estabilidade, o que os torna interessantes para terapia fotodinâmica, imagiologia celular, transporte de fármacos, mas também como materiais fotovoltaicos orgânicos.

Este trabalho teve como objetivo sintetizar e caracterizar novos BODIPYs aromáticos e alifáticos e, posteriormente, avaliar sua atividade biológica em estudos in vitro, para o uso posterior em terapia fotodinâmica.

A síntese de BODIPYs envolve a condensação de um alfa-livre pirrole e aldeídos na presença de um ácido, formando um intermediário, o dipirrometano que é oxidado a dipirrometeno. Em seguida, o dipirrometeno é complexado com trifluoreto de boro na presença de uma base. A troca de solvente, de diclorometano para tetrahidrofurano torna o procedimento quimicamente mais verde leva a melhores rendimentos. O estudo da possibilidade de realizar a foto-oxidação do dipirometano ao invés da usual oxidação química com DDQ, também foi estudada.

Todos os BODIPYs sintetizados foram caracterizados por RMN, espectroscopia de absorção e emissão e espectrometria de massa. O dímero BODIPY e o Meso-Fenil-BODIPY foram estudados como potenciais fotossensibilizadores em PDT em duas linhas celulares do cancro do pulmão, H1299 e A549. A citotoxicidade e a fototoxicidade usando o ensaio MTT foram avaliadas após 24 e 48h. O dímero BODIPY não apresentou citotoxicidade ou fototoxicidade para todas as condições, no entanto, o Meso-Fenil-BODIPY mostrou-se citotóxico para concentrações mais altas e mostrou fototoxicidade na linha celular A549.

Em resumo, o estudo atual forneceu bons resultados sobre a síntese de BODIPY com avanços consideráveis em termos de otimização de processo, com resultados comprovados de testes de laboratório primários em células do cancro do pulmão. Com base nos resultados, o dímero pode ser um bom candidato para diagnóstico, uma vez que não é tóxico e o Meso-Fenil BODIPY é um candidato para PDT.

Palavras-chave: BODIPY, síntese orgânica, foto-oxidação, terapia fotodinâmica

Chapter 1

1-Introduction

1.1-Medicinal Chemistry

Medicinal chemistry is a relevant area of chemistry, notably where synthetic organic chemistry[1], pharmacology[2] and various other biological specialties[3], are involved in the design, the chemical synthesis, and the development for market of pharmaceutical agents, or bio-active molecules, commonly termed drugs.[4]

Compounds used as medicines are often organic compounds, which are commonly divided into the broad classes of small organic molecules (e.g., atorvastatin[5], fluticasone[6], clopidogrel[7]), shown in figure 1, and biologic (infliximab[8], erythropoietin[9] , insulin glargine[10]) shown in figure 2, the latter of which are most often medicinal preparations of proteins (natural and recombinant antibodies, hormones, among other).

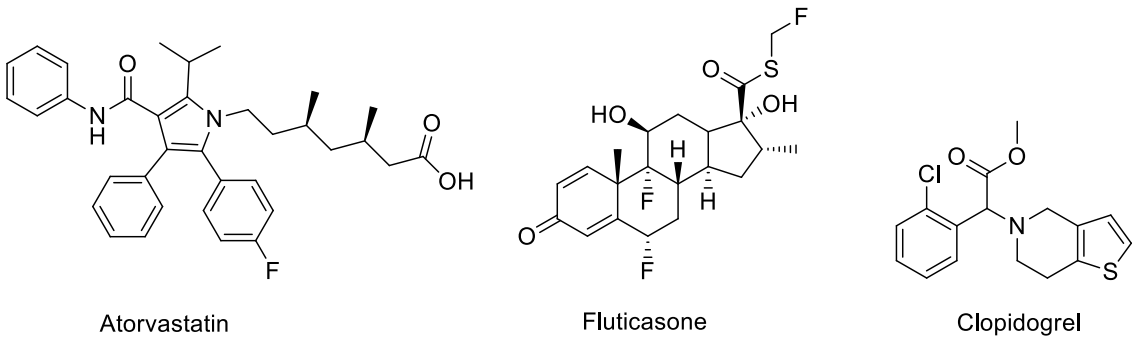

Figure 1- Molecular structure of Atorvastatin, Fluticasone and Clopidogrel.

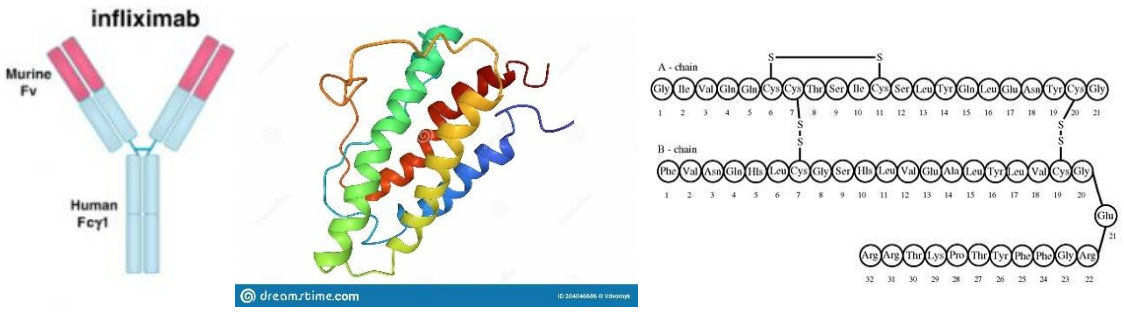

Figure 2- Structures of Infliximab, erythropoietin, and insulin glargine

Inorganic and organometallic compounds are also useful as drugs (e.g., lithium and platinum-based agents such as lithium carbonate and cisplatin as well as gallium)[11] (Figure 3).

Figure 3- Chemical structure of lithium carborate and cisplatin.

Medicinal chemistry in its most essential practice focuses on small organic molecules, which encompasses synthetic organic chemistry and aspects of natural products and computational chemistry in close combination with chemical biology, enzymology, and structural biology, aiming at the discovery and development of new therapeutic agents. Essentially, it involves chemical aspects of identification, and then systematic, thorough synthetic alteration of new chemical entities to make them adequate for therapeutic use. It recently includes synthetic and computational aspects[12] of the study of existing drugs and agents in development in relation to their bioactivities (biological activities and properties), i.e., understanding their structure–activity relationships (SAR). [13]

Medicinal chemistry is an area of study that exponentially evolved in the past few years currently representing one of the most important fields of study.[14] . The many subjects involved, such as diseases, from tropical diseases [15] to the most common, antiviral and viral studies (e.g. viral polymerases for antiviral therapy[16], coronavirus[17], Monkeypox[18]), to every type of cancer are studied and each year more and more development is achieved.

1.2-Photodynamic Therapy

According to the Global Cancer Observatory (GCO), cancer is a leading cause of death worldwide, accounting for nearly 10 million deaths in 2020 [19]. Furthermore, the number of new cases of liver cancer per year is predicted to increase by 55.0%

between 2020 and 2040, with a possible 1.4 million people diagnosed in 2040. A predicted 1.3 million people could die from liver cancer in 2040 (56.4% more than in 2020).[20] The established standard treatment strategies (surgery, radiotherapy, and chemotherapy) have demonstrated reasonable success for specific cancers in recent years. Despite this, some issues such as resistant cancer cells, recurrence, and metastases has not yet been overcome. For this reason, new technologies are essential for future cancer treatments.[21]

A non-conventional therapeutic modality for solid tumours, which offers advantages over standard treatments, is a light based technology named photodynamic therapy (PDT) [22]. Light has been used in medical treatments for over a millennium. It was used in ancient Egypt, India, and China to treat skin diseases, such as psoriasis, vitiligo, and cancer, as well as rickets and even psychosis [23] . Despite this, sunlight as a medical treatment was not widely used until the eighteenth century. The Nobel Prize awarded to Niels Finsen acknowledged phototherapy in 1903. He was granted this prize for treating cutaneous tuberculosis by using ultraviolet light.

Simultaneously, J. Prime discovered that patients with epilepsy treated orally with eosin were sensitive to the sun on exposed areas of the skin, causing dermatitis [21]. Thanks to this discovery, H. Tappeiner and A. Jesionek employed a topical version of eosin along with a white light source to treat skin tumours [24] . After that, the term ‘‘photodynamic action’’ was coined by H. Tappeiner and A. Jodlbauer when they discovered the oxygen requirement in photosensitization reactions [25]. After this work, little research was performed until 1972. In this year, Diamond et al. achieved a reduction of tumour growth for some days using porphyrins as photosensitising agents [26], concluding that photodynamic action (renamed to photodynamic therapy, PDT) could be used as a new approach to treat this disease. In 1975, the first significant milestone in PDT occurred at the Roswell Park Cancer Institute in Buffalo. T. J. Dougherty et al. reported the first successful complete tumour cure in animal specimens by using more than 600 nm light 24 or 48 hours after an injection of hematoporphyrin [27], starting a new era for Photodynamic Therapy. The first PDT clinical trials date back to the late 1970s [28] . In that study, the effects of light and hematoporphyrin derivative (HpD) in five patients with bladder cancer were studied. Later in 1978, Dougherty reported the first large series of patients successfully treated with PDT [29]. Several types of tumours were analysed, and all of them demonstrated a response to the treatment.

Photodynamic therapy involves administration of a tumour-localizing photosensitizing agent, which may require metabolic synthesis (i.e., a prodrug), followed by activation of the agent by light of a specific wavelength. This therapy results in a sequence of photochemical and photobiologic processes that cause irreversible photodamage to tumour tissues.

Ideally there are many aspects that a photosensitizer must have, high chemical purity, an easy synthesis with high yields, low toxicity in the dark, high molar absorption coefficient in the therapeutic window (600 - 850 nm) and appropriate photophysical properties, including low fluorescence yield, high singlet oxygen production and long triplet half-life state and at least a good dissolution in biocompatible formulations.

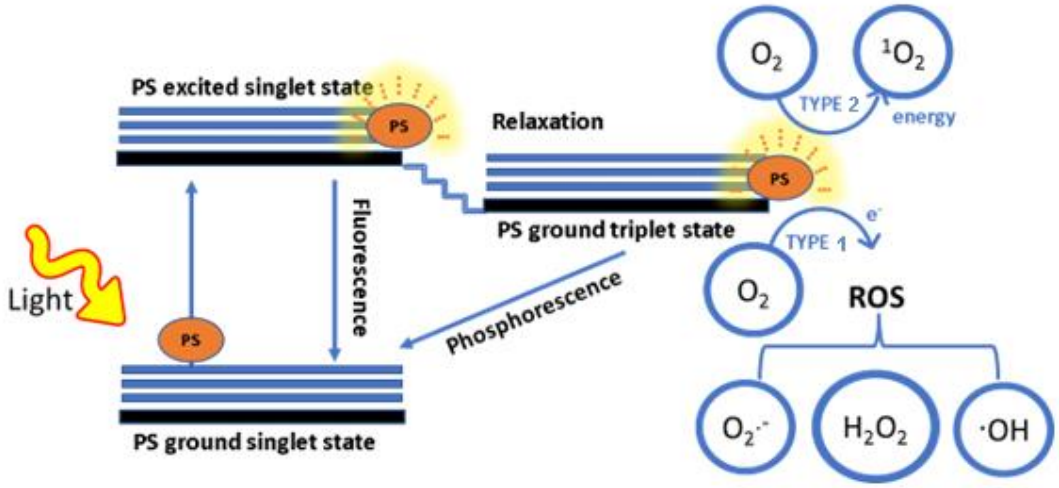

Figure 4- Photodynamic Therapy scheme (adapted from [30]).

Schematically, as seen in Figure 4, after excitation by light, the photosensitizer passes from ground state to the excited singlet state. The excited state of the photosensitizer is very unstable. It can decay to the ground state, through emission of fluorescence and/or heat, without photodynamic effect, or pass to the metastable triplet state. In this state, it can decay back to the ground state through the emission of phosphorescence or transfer its energy to molecular oxygen $^3(O_2)$ whose ground state is triplet. This second process leads to the formation of the excited state of singlet oxygen $^1(O_2)$ that will react with nearby biomolecules and lead to the destruction of

cancerous tissues, in a photodynamic reaction called type II. In the type I photodynamic reaction, the triplet state interacts with cellular substrates and forms free radicals, which interact with molecular oxygen and forms reactive oxygen species (peroxides, superoxide ions and hydroxyl radicals). These can oxidize a variety of biomolecules, especially amino acids and unsaturated lipids, compromising their biological functions.[31] The accumulation of reactive oxygen species results in oxidative stress and thus, cell death by apoptosis, necrosis and sometimes cell death associated with autophagy.[32] In photodynamic therapy, most photosensitizers trigger type II reactions.[33][34]

PDT as a medical methodology has already proven its ability to kill cancer cells, bacteria, fungi and viruses. It is also used in the treatment of acne and age-related macular degeneration, psoriasis, atherosclerosis and has shown some effectiveness in antiviral treatments. [35] [36]

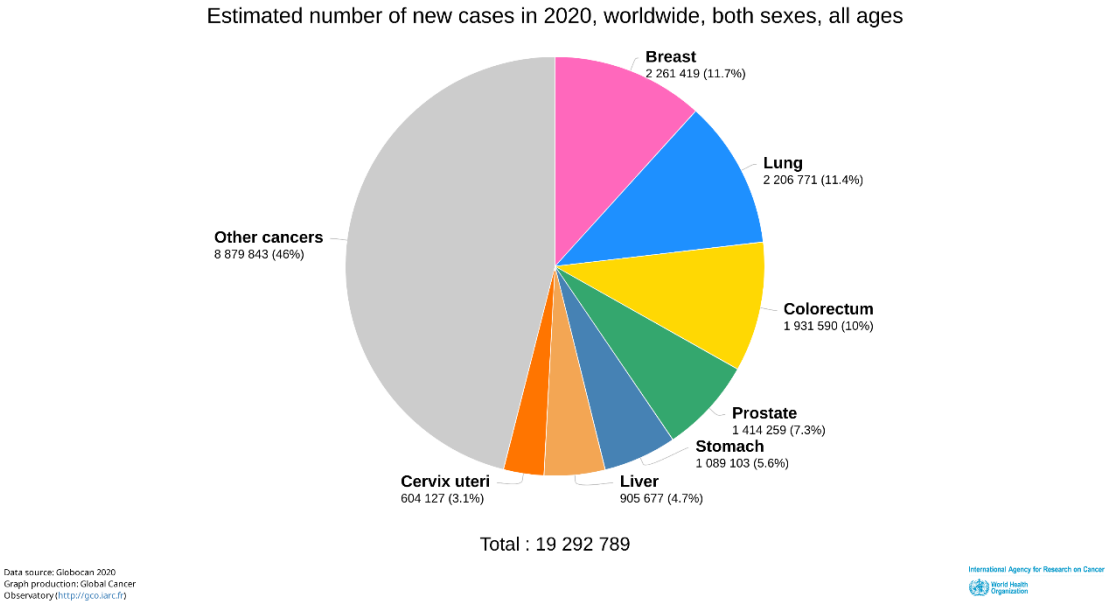

Figure 5- Chart of the estimated number of new cases in 2020.[19]

Lung cancer consists of a group of diseases resulting from the malignant growth of cells of the respiratory tract, particularly lung tissue, and is one of the most common types of cancer worldwide.[19] Lung cancer usually originates from epithelial cells and can lead to metastasis and infiltration on other body tissues. PDT can be used for early-stage lung cancer, advanced lung cancer with airway obstruction, or preoperative procedures.[21]

1.3-BODIPY Molecules

Since their discovery in 1964, BODIPYs have been an important line of chemical research. Successive research works in the Chemistry of BODIPYs, like the works of Burgess et al. 2007 [37] and Ziessel et al. 2007 [38] and 2008 [39] , which cover in detail the various synthesis techniques, core modifications and applications up to the most recent work by Shen et al. 2014 [40] and Boens, Dehaen et al. 2015 [41] who respectively describe the synthesis of BODIPYs emitting in the near-infrared (NIR) and the functioning of BODIPYs in advanced stages.

The last 10 years have seen considerable advances in the development and optimization of synthesis pathways and functional architectures of BODIPYs contributing to the popularity of these valuable fluorophores. [42]

The photochemical characteristics of the chemical manipulations of the BODIPY core result in three types of reactions, through the addition of substituents to the BODIPY core, they are substitution, functional group inter-conversion and metal-catalysed cross-coupling reaction, which represent numerous applicability interests. [43]

Some of the applications, in the most diverse areas, are for example in ion/molecule probes, PH probes, chelating agents, conjugation groups for biomolecules, photosensitizers for photodynamic therapy, drug delivery agents, laser dyes and organic solar cells. [44]

More recently, the study of BODIPYs has progressed a lot at the University of Coimbra, one of the main studies being to improve the lipophilicity of BODIPYs by adding lipophilic chains without disturbing their excellent fluorescent properties [45]. Another study uses BODIPYs as a simple and reliable method with fast response for detection and quantification of lipids, using a new method of image analysis to determine lipid content in algae and lipid production in microalgae for biofuel production [46]. As a last study, the synthesis, characterization and application of meso-substituted BODIPYs in organic photovoltaic cells [47].

BODIPY is an abbreviation used to describe boron-complexed dipyrromethenes (hence the name BOron DIPYrromethenes), which are compounds of the organoboride family. In fact, BODIPY is composed of a dipyrromethene unit complexed with a disubstituted boron centre, typically BF_2. The IUPAC name for the BODIPY skeleton is 4,4-difluoro-4-bora-3a, 4a-diaza-s-indacene [48] (figure 5).

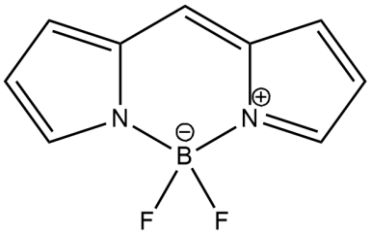

Figure 6- 4,4-difluoro-4-bora-3a,4a-diaza-s-indacene.

BODIPYs were discovered in 1968 by Treibs and Kreuzer. BODIPYs present 3 types of peripheral positions (meso, alpha and beta) as shown in figure 6, and have resonance forms that favour a negative character in boron and a positive character in the nitrogen of the pyrrole rings [24].

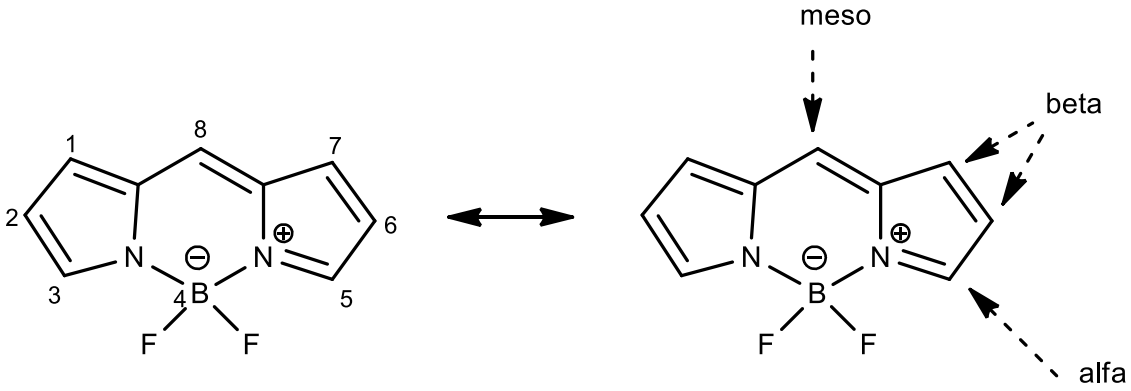

Figure 7- Positions and nomenclature of BODIPYs molecules.

BODIPYs absorb light in the visible range and are often characterized by strong absorption and emission spectra with high molar extinction coefficients, high fluorescence quantum yields, and narrow absorption and emission bandwidths.

BODIPY dyes and its derivatives are highly adaptable due to their versatile nature, thus have a multifunctional application in photodynamic therapy. BODIPY dyes can act as a photosensitizer and undergo structural modifications that make them worthwhile alternatives for photodynamic therapy without reporting any side effects to healthy cells.[49]

There are many studies using BODIPYs as a photosensitizer, most of them focus on BODIPY core modifications to facilitate singlet oxygen generation. The absorption of simple BODIPY dyes is between 510–530 nm, this is shorter than ideal, so many of the featured modifications also aim to extend conjugation in these molecules, making them better photosensitizing agents.[44]

Chapter 2

Experimental

2.1- Reagents and solvents

Reagents and solvents were obtained from Sigma-Aldrich and used without further purification. Solvents for photophysical studies were HPLC grade (CHROMASOLV plus) purchased from Sigma-Aldrich. Analytical thin-layer chromatography (TLC) was performed on silica gel plates with F-254 indicator (Merck). Visualization was accomplished by a twin wavelength ultraviolet lamp (254 and 365 nm). Silica gel column chromatography was carried out with silica gel (230–400 mesh) from Fluka. Preparative thin layer chromatography was performed using 20 x 20 cm glass plates and silica gel 60G from Fluka.

2.2- Instrumentation

2.2.1- Mass spectrometry

The studies were made in a mass spectrometer THERMOSCIENTIFIC, model LXQ, with ESI mode. The compounds were dissolved in dichloromethane and diluted in acidified methanol with 0.1% of formic acid, MS grade. All solvents were HPLC grade.

2.2.2- Nuclear Magnetic Resonance Spectroscopy

^{1}H, ^{13}C, ^{19}F and ^{11}B NMR spectra were acquired in a Bruker AVANCE III NMR (running at 400 MHz for proton, 100 MHz for carbon, and 376 MHz for fluorine) with $CDCl_3$ as solvent. The solvent protons were used as internal standards. The coupling constants were calculated using the chemical shifts with three decimal places.

2.2.3- UV-vis spectroscopy

The studies were made in a UV-vis Spectrophotometer Shimadzu UV-2600 and was studied the absorption of the compounds in a wavelength between 200 nm and 800 nm.

2.2.4- Spectrofluorometer

The spectrofluorometer used was Fluoromax-4 and it was used to irradiate the solution in a specific wavelength, mainly in the UV region.

2.3 Synthetic procedures

2.3.1 Procedure for the synthesis of BODIPYs 1 using DCM

Distilled dichloromethane (30 mL) was purged with nitrogen for 10 minutes. Terephthaldehyde (0.9mmol, 0.256g) and 3-ethyl-2,5-dimethyl-pyrrole (3.7 mmol, 1 mL) with 1:4 stoichiometry was added to dichloromethane. Trifluoracetic acid (3 to 4 drops) was added to the solution and was stirred for 30 minutes at room temperature under N_2 atmosphere. After that, 2,3-dichloro-5,6- dicyano-1,4-benzoquinone (DDQ) (1.8mmol, 0.8g) was added to the reaction mixture and was stirred for 30 minutes.
Then N,N-diisopropylethylamine (12 eq.) and $BF_3.Et_2O$ (17 eq.) were added to the solution for 30 minutes. The final reaction mixture was washed with water (30 mL) and brine (30 mL). The organic layer was dried with anhydrous sodium sulphate and concentrated under reduced pressure.

The compound was isolated by column chromatography on silica gel, using CH_2Cl_2: Hexane 1:1 as solvent. BODIPY 2 was found as a by-product of this synthesis.

10,10'-(1,4-phenylene)bis(2,8-diethyl-5,5-difluoro-1,3,7,9-tetramethyl-5H-dipyrrolo[1,2-c:2',1'-f][1,3,2]diazaborinin-4-ium-5-uide) (BODIPY 1)

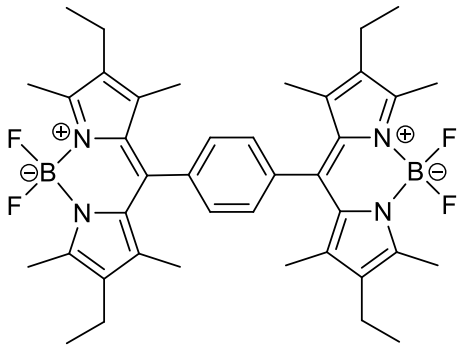

^{1}H NMR (400 MHz, $CDCl_3$) δ (ppm): 7.51 (s; 4H); 2.56 (s, 12H), 2.32 (q, J = 7.6 Hz, 8H), 1.48 (s, 12H), 1.00 (t, J = 7.6 Hz, 12H);

HRMS m/z $[M+H]^+$ calculated for $C_{40}H_{48}B_2F_4N_4^+$: 683.45; Found: 683.6

2,8-diethyl-5,5-difluoro-1,3,7,9-tetramethyl-5H-dipyrrolo[1,2-c:2',1'-f][1,3,2]diazaborinin-4-ium-5- uide (BODIPY 2)

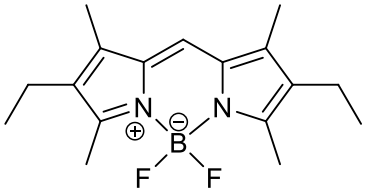

^{1}H NMR (400 MHz, $CDCl_3$) δ (ppm): 6.94 (s; 1H); 2.49 (s, 6H), 2.38 (q, J = 7.6 Hz, 4H), 2.17 (s, 6H), 1.06 (t, J = 7.6 Hz, 6H);

HRMS m/z $[M+H]^+$ calculated for $C_{17}H_{23}BF_2N_2^+$: 305.2; Found: 305.3

2.3.2 General procedures for the synthesis of BODIPY 1, 3 and 4 using THF

The experimental procedure followed was the described in the subchapter 2.3.1. The difference was the change of solvent, in this case, tetrahydrofuran was used to replace dichloromethane. Benzaldehyde and benzene-1,3,5-carboxaldehyde (1.8 mmol) were used as aldehydes to form BODIPY 3 and 4, respectively.

10,10'-(1,4-phenylene)bis(2,8-diethyl-5,5-difluoro-1,3,7,9-tetramethyl-5H-dipyrrolo[1,2-c:2',1'-f][1,3,2]diazaborinin-4-ium-5-uide) (BODIPY 1)

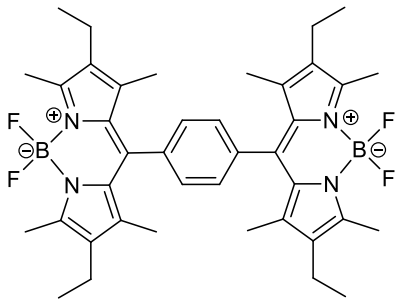

^{1}H NMR (400 MHz, $CDCl_3$) δ (ppm): 6.94 (s; 1H); 2.49 (s, 6H), 2.38 (q, J = 7.6 Hz, 4H), 1.48 (s, 12H), 1.00 (t, J = 7.6 Hz, 12H)

^{13}C NMR (100 MHz, $CDCl_3$): 153.68; 138.42; 136.81; 132.97; 129.01; 17.12; 14.61; 13.27; 12.64

^{19}F NMR (376 MHz, $CDCl_3$) δ (ppm): -145.80 (q, J = 33.46 Hz, 4F)

^{11}B NMR (128 MHz, $CDCl_3$) δ (ppm): 0.77 (t, J = 33.28 Hz)

2,8-diethyl-5,5-difluoro-1,3,7,9-tetramethyl-10-phenyl- 5H-dipyrrolo[1,2-c:2',1'-f] [1,3,2] diazaborinin-4-ium-5- uide (BODIPY 3)

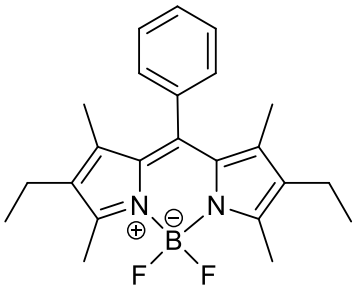

^{1}H NMR (400 MHz, $CDCl_3$) δ (ppm): 7.47 (t; 3H); 7.28 (d; 2H); 2.53 (s, 6H), 2.30 (q, J = 7.6 Hz, 4H), 1.26 (s, 6H), 0.98 (t, J = 7.6 Hz, 6H)

^{13}C NMR (100 MHz, $CDCl_3$): 128.14; 127.90; 127.34; 16.21; 13.73; 10.68

^{11}B NMR (128 MHz, $CDCl_3$) δ (ppm): 0.80 (t, J = 33.28 Hz).

^{19}F NMR (376 MHz, $CDCl_3$) δ (ppm): -145.80 (q, J = 33.46 Hz, 2F).

HRMS m/z $[M+H]^+$ calculated for $C_{23}H_{28}BF_2N_2^+$: 381.3; Found: 381.4

10,10',10''-(benzene-1,3,5-triyl)tris(2,8-diethyl-5,5- difluoro-1,3,7,9-tetramethyl-5H-di pyrrolo[1,2-c:2',1'- f][1,3,2]diazaborinin-4-ium-5-uide) (BODIPY 4)

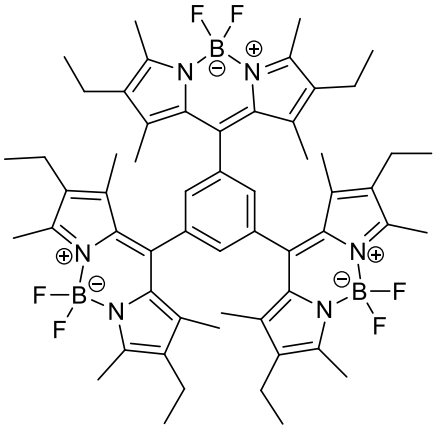

^{1}H NMR (400 MHz, $CDCl_3$) δ (ppm): 7.74 (s; 3H); 2.54 (s, 18H), 2.31 (q, J = 7.6 Hz, 12H), 1.69 (s, 18H), 1.01 (t, J = 7.6 Hz, 18H)

HRMS m/z $[M+H]^+$ calculated for $C_{57}H_{69}B_3F_6N_6{}^+$: 985.6; Found: 985.7

2.3.3 Bromination of BODIPY 1

BODIPY (0.026mM) and NBS (0.026mM, 4.7 mg) (1:1) stoichiometry were added in 3 mL of THF with an increment of 10% of NBS. The reaction mixture was stirred at room temperature for 72 hours for BODIPY 1. After that, the solution was heated in water bath at 40°C. The products formed were analysed by TLC and absorption spectra.

2.3.4 General procedures for the synthesis of BODIPY 6 and 7

Aliphatic aldehyde (1.8 mmol) and 3-ethyl-2,5-dimethyl-pyrrole (3.7 mmol, 1 mL) with 1:2 stoichiometry was added to tetrahydrofuran. Trifluoracetic acid (3 to 4 drops) was added to the solution and was stirred for 30 minutes at room temperature under N_2 atmosphere. After that, 2,3-dichloro-5,6- dicyano-1,4-benzoquinone (DDQ) (0.9 mmol, 0.4 g) was added to the reaction mixture and was stirred for 15 minutes.

Then N,N-diisopropylethylamine (12 eq.) and $BF_3.Et_2O$ (17 eq.) were added to the solution for 15 minutes. The final reaction mixture was washed with water (30 mL) and brine (30 mL). The organic layer was dried with anhydrous sodium sulphate and concentrated under reduced pressure. The products were isolated by column chromatography on silica gel, using CH_2Cl_2: Hexane 1:1 as solvent.

2,8-diethyl-5,5-difluoro-10-isopropyl-1,3,7,9-tetramethyl-5H-dipyrrolo[1,2-c:2',1'-f][1,3,2]diazaborinin-4-ium-5-uide (BODIPY 6)

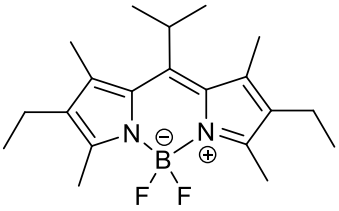

^{1}H NMR (400 MHz, $CDCl_3$) δ (ppm): 2.49 (s, 6H), 2.38 (q, J = 7.6 Hz, 4H), 2.18 (s, 12H); 1.48 (s, 12H), 1.05 (t, J = 7.6 Hz, 12H)

^{11}B NMR (128 MHz, $CDCl_3$) δ (ppm): 0.49 (t, J = 33.28 Hz).

^{19}F NMR (376 MHz, $CDCl_3$) δ (ppm): -145.85 (q, J = 33.46 Hz, 2F); -146.33 (q, J = 33.46 Hz, 2F)

HRMS m/z $[M+H]^+$ calculated for $C_{20}H_{29}BF_2N_2^+$: 347.3; Found: 347.4

2,8-diethyl-5,5-difluoro-1,3,7,9,10-pentamethyl-5H-dipyrrolo[1,2-c:2',1'-f][1,3,2] diazaborinin-4-ium-5-uide (BODIPY 7)

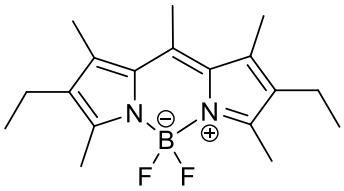

^{1}H NMR (400 MHz, $CDCl_3$) δ (ppm): 2.49 (s, 6H), 2.38 (q, J = 7.6 Hz, 4H), 2.17 (s, 3H), 1.29 (s, 6H), 1.06 (t, J = 7.6 Hz, 6H)

HRMS m/z $[M+H]^+$ calculated for $C_{18}H_{25}BF_2N_2^+$: 319.3 m/z

2.4 *In vitro* studies

A549 (ATCC CCL-185, human alveolar basal epithelial adenocarcinoma cells) and H1299 (ATCC CRL-5803, human non-small cell lung carcinoma cells) were the two cell lines where BODIPYs were tested. The cell lines were propagated in a humidified atmosphere with 95% air and 5% CO_2, at a temperature of 37°C in a HeraCell incubator. The culture medium used was Dulbecco's Modified Eagle Medium (DMEM, Sigma Aldrich®, USA), supplemented with a 5% of Fetal Bovine Serum (FBS, from English Foetal Bovine Serum, Sigma Aldrich®, USA), sodium pyruvate and antibiotic (Antibiotic Antimycotic Solution, Sigma Aldrich®, USA), respecting the supplier's instructions. The cells were detached from the culture flasks using TrypLE ExpressTM (2 mL) and incubated for 5 minutes at 37°C. After, 4 mL of culture medium was added to the cell to inactivate the TrypLE, and the mixture was homogenized. A mixture of Trypan Blue solution and cell suspension, in equal amounts, was prepared and transferred to a hemocytometer. Using inverted optical microscopy, the number of living cells was calculated. BODIPY 1 and 3 solutions were prepared in dimethylformamide and dimethylsulfoxide, respectively, and tested in concentrations between 1 and 100 µM.

2.4.1 Photodynamic Therapy

Cell suspension of about 100,000 cells/mL was incubated in 48-well plates overnight to allow cell adhesion. BODIPYs concentrations were applied at concentrations from 1 to 100 µM. After 24 hours, the culture medium was removed, and the cells were washed with phosphate-buffered saline (PBS) and added medium. The cells were exposed to irradiation with a flux of 7.5 mW/cm^2 until reaching a total of 10 J, with a red light (λ>570 nm). In parallel, cell cultures were just incubated in the dark with the BODIPYs with any irradiation. In all experiments, two controls were used: cells that had not been treated and cells that had been treated with the solvent used in solutions.

2.4.2 MTT assay

The MTT (3-(4,5-Dimethyl-thiazolyl-2)-2,5-diphenyl-tetrazolium bromide) assay is a colorimetric assay that measures the metabolic activity of cells. The assay is based on the ability of metabolically active cells to reduce the soluble salt of tetrazolium (MTT)

(yellow) in formazan crystals (water-insoluble dark violet product), as represented in Figure 15. This reduction process is associated with the function of mitochondrial dehydrogenases. However, it may also be due to the action of molecules such as NADH and NADPH (reducing equivalents).

After an incubation of 24 and 48 hours, the culture medium was removed from the cells and washed with PBS. Cells were incubated with 100 µL MTT in PBS (pH=7.4) for 2h30. After the incubation period, the insoluble crystals of formazan were dissolved in 200 µL of a solution of 0.04M HCl in isopropanol. Absorbance was determined at a wavelength of 570 nm, using the wavelength of 620 nm as a reference, on the Enspire® spectrophotometer. To calculate the percentage of metabolic activity was used the following equation:

$$\%Metabolic\ Activity = \frac{(\text{Treated Cells with BODIPY})(\text{Abs } 570\text{nm} - \text{Abs } 620\text{nm})}{(\text{Treated Cells with Solvent})(\text{Abs } 570\text{nm} - \text{Abs } 620\text{nm})} \times 100$$

Chapter 3

Results and Discussion

3.1 Synthesis of Aromatic BODIPYs

As mentioned in the introduction, different methods are used to prepare BODIPYs. The method used in this experimental work is the conventional synthesis constituted by three steps. First, the condensation of aromatic aldehydes and pyrroles with one position free were catalysed by acid, followed by DDQ oxidation, and finally, the complexation with boron trifluoride in the presence of a base, as shown in the scheme 1.

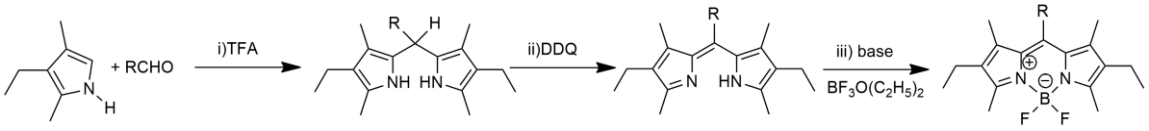

Scheme 1- Synthesis of a BODIPY from a pyrrole molecule and an aldehyde.

Using this method, we synthesized four BODIPY from aromatic aldehydes (terephthaldehyde, benzaldehyde and benzene-1,3,5-carboxaldehyde), being one of them a by-product, and which were characterized by NMR, absorbance fluorescence and mass spectra. In this subchapter, the study of change of solvent was analysed, as well as the bromination reaction of BODIPYs.

3.1.1 Synthesis of BODIPY dimer (BODIPY 1) using DCM

The synthesis of the BODIPY dimer, presented in the scheme 2, was controlled by TLC. After purification by chromatography column with 1:1 dichloromethane: hexane as a solvent, two compounds were obtained as shown in the TLC from the figure 8. The TLC A-C using DCM: Hex 1:1 as solvent, represented the BODIPY dimer (left side) and the core (right side) on each TLC, under two different UV lights (A and B) and iodine (C). Images D and E correspond to a two-dimensional TLC made in DCM: Hex 1:1 and chloroform in the opposite direction. These results showed that the two compounds separated are different, being that more visible under UV light (E).

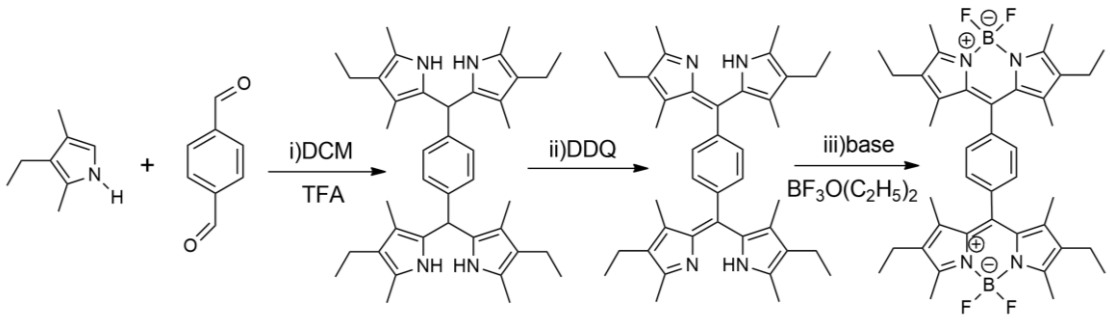

Scheme 2- Synthesis of the BODIPY dimer.

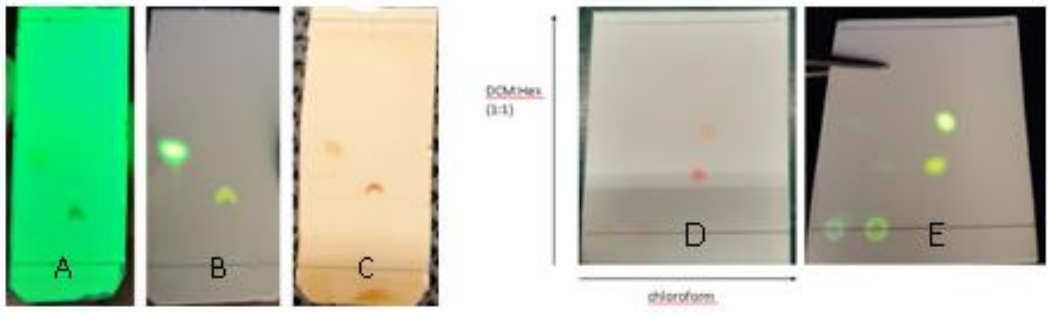

Figure 8- TLC and bidimensional TLC of the dimer and the core.

This analysis is not a 100% confirmation of purity, once only gives the idea of different compounds possibly existing with different polarity and/ or size, other characterization methods are needed to identify the molecules.

Analysing the ^{1}H NMR spectrum it was possible to identify the BODIPY dimer (figure 9). The symmetric molecule has an ethyl group corresponding to a triplet and a multiplet at 1.0 and 2.32 ppm, and two methyl groups represented by two singlets at 2.56 and 1.48 ppm. The significant difference in ppm of the singlet is due to the protection of the hydrogens, being near an aromatic group more specifically the phenyl group, deflected to the right of the spectrum and the proximity of nitrogen deflects the peaks to the left. The singlet at 7.51 ppm is of the phenyl group because all protons are equivalent. The peak of deuterated chloroform at 7.26 ppm, water at 1.56 ppm, and hexane at 0.88 and 1.26 ppm were also identified.[47]

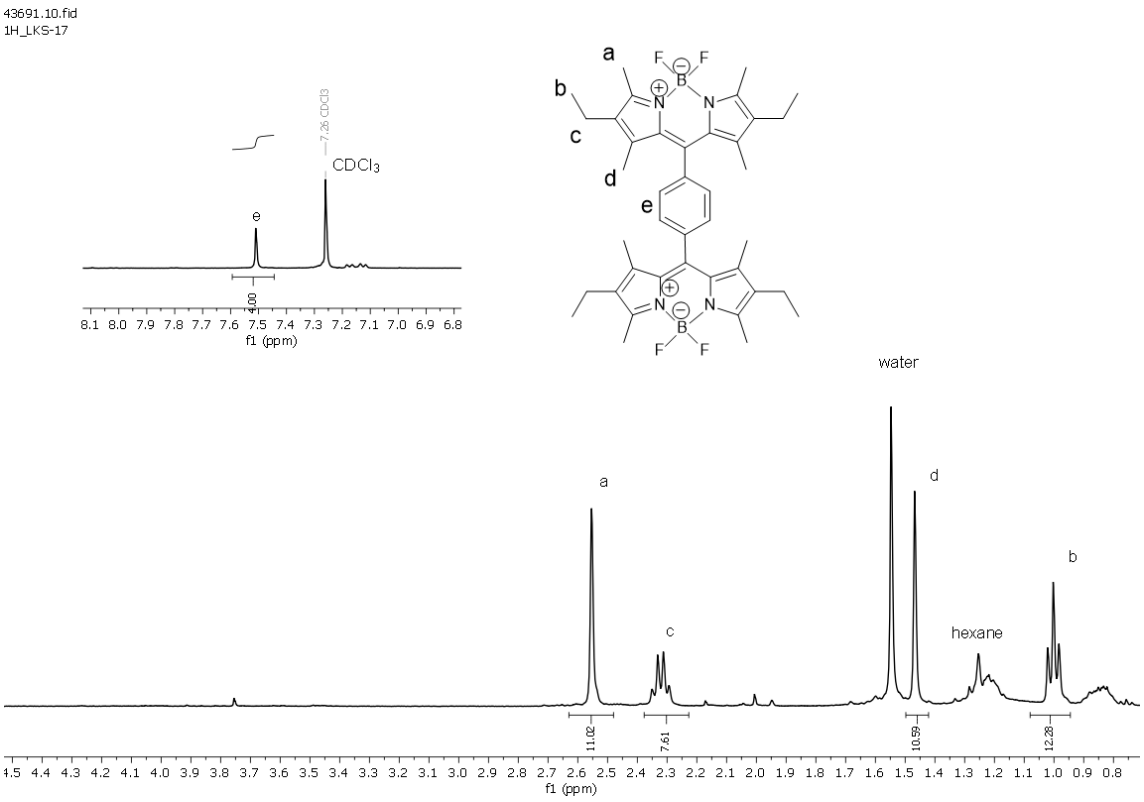

Figure 9 - ^{1}H NMR spectrum of BODIPY dimer.

^{1}H NMR (400 MHz, $CDCl_3$) δ (ppm): 7.51 (s; 4H); 2.56 (s, 12H), 2.32 (q, J = 7.6 Hz, 8H), 1.48 (s, 12H), 1.00 (t, J = 7.6 Hz, 12H)

After the chromatographic separation it was possible to isolate the by-product, the BODIPY core. The analysis by ^{1}H NMR allowed identifying the core, a by-product of this synthesis when dichloromethane was used as the solvent (figure 10). The BODIPY core presented two methyl groups identified by the singlets at 2.49 and 2.17 ppm, one ethyl group represented by a triplet at 1.06 ppm and a quadruplet at 2.38 ppm. The peak at 6.94 ppm corresponded to the hydrogen in the meso position of the BODIPY. The solvents' peaks are also detected. [47]

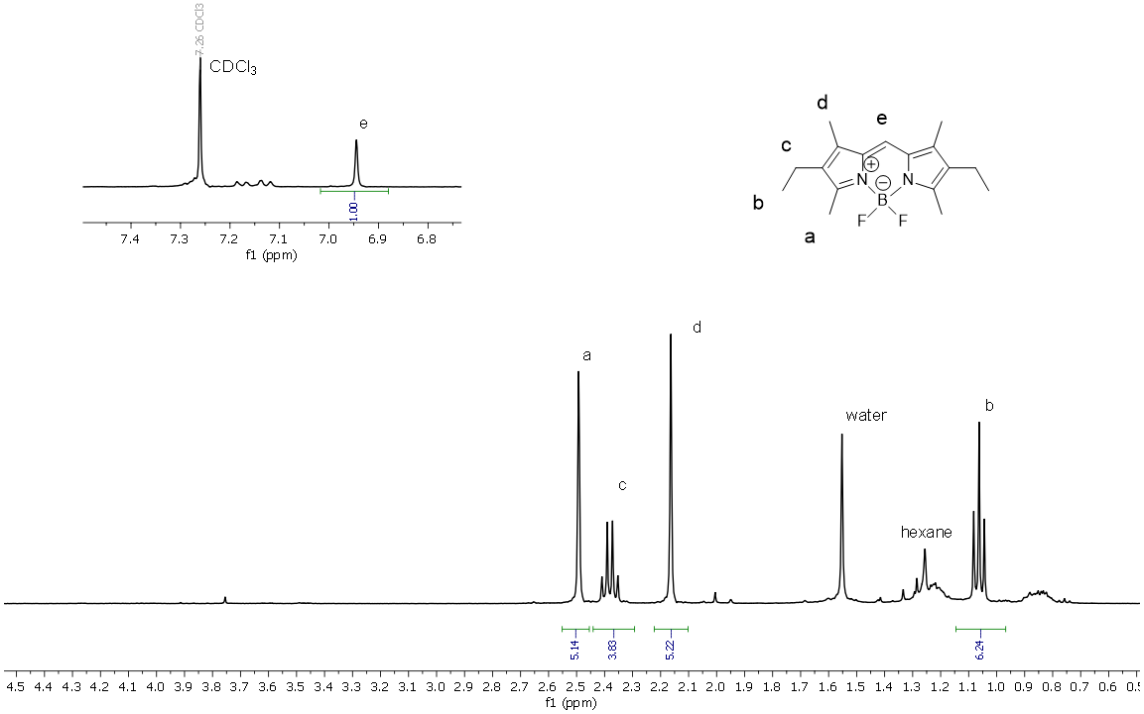

Figure 10 - ^{1}H NMR spectrum of the core.

^{1}H NMR (400 MHz, $CDCl_3$) δ (ppm): 6.94 (s; 1H); 2.49 (s, 6H), 2.38 (q, J = 7.6 Hz, 4H), 2.17 (s, 6H), 1.06 (t, J = 7.6 Hz, 6H)

Both molecules were also characterized by mass spectrometry. Figure 11 shows, the identification of peaks of BODIPY dimer protonated $[M+H]^{+\cdot}$, dimer without a fluor (F) and the dimer without hydrogen fluoride (-HF). There are peaks corresponding to the core at 304.4 and the BODIPY with a phenyl group in the meso position at 381.4 (Figure 12). One very common peak in BODIPY mass spectra is the BODIPY dimer with iron at 707.6.

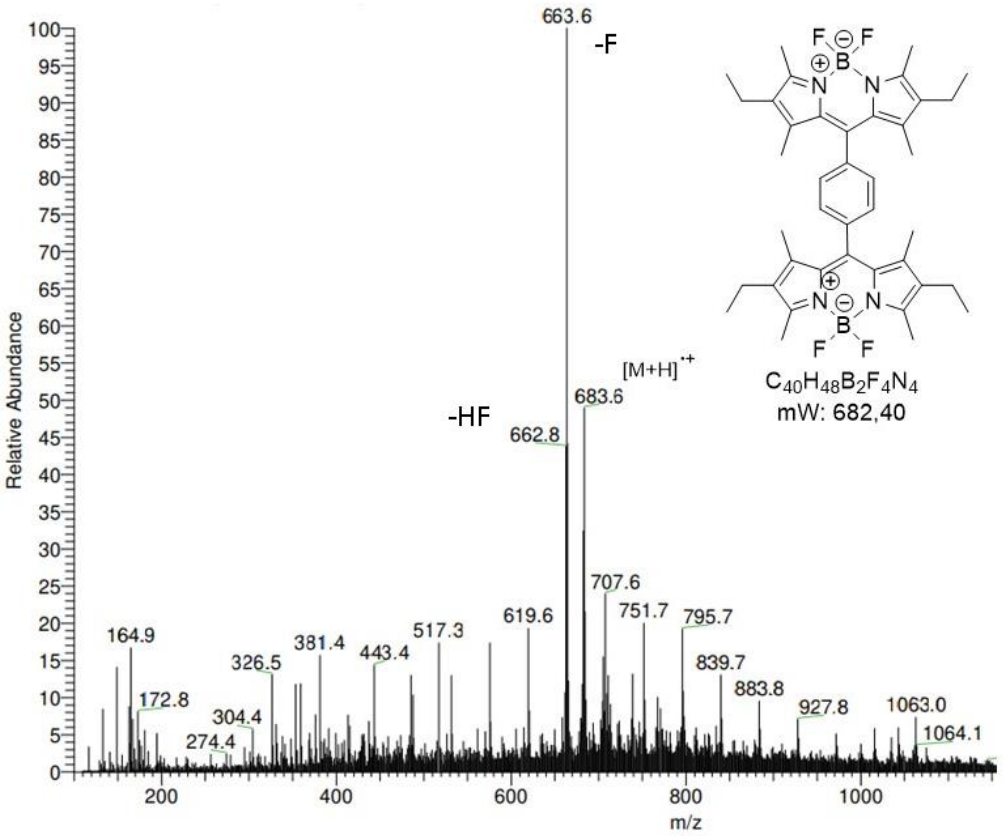

Figure 11- Mass spectrum of the BODIPY dimer.

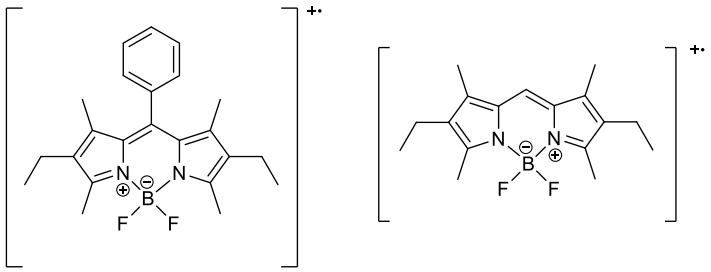

Figure 12- Chemical structure of fragments representing the core and phenyl-BODIPY.

In figure 13, another mass spectrum of the peak 683.5 was performed, giving all possible fragmentations of the BODIPY dimer. The more abundant peaks were the fragmentations of a methyl group, fluorine, and an ethyl group, confirming our previous explanation in the figure below.

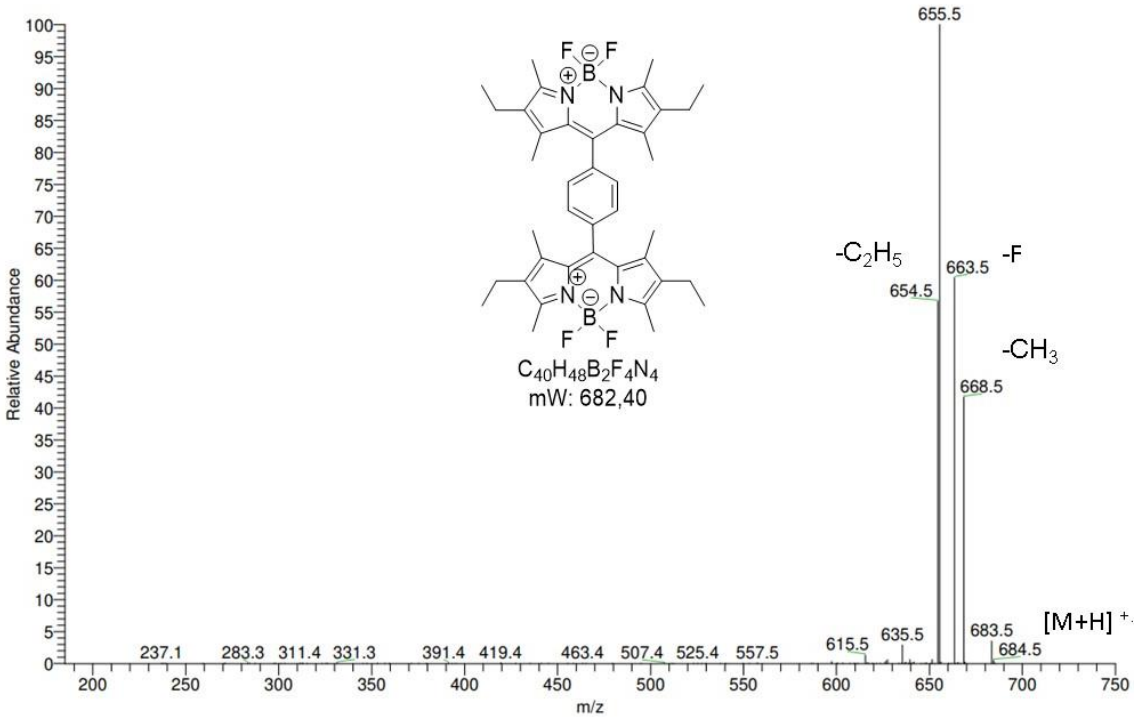

Figure 13 - Mass spectrum of the fragment 683.5 m/z.

In the following mass spectrum (figure 14), the mass of the core can be detected at 305.3 m/z. Another characteristic peak found in many BODIPY compounds is at 285.3 m/z that represents the core without a hydrogen fluoride (-HF) group.

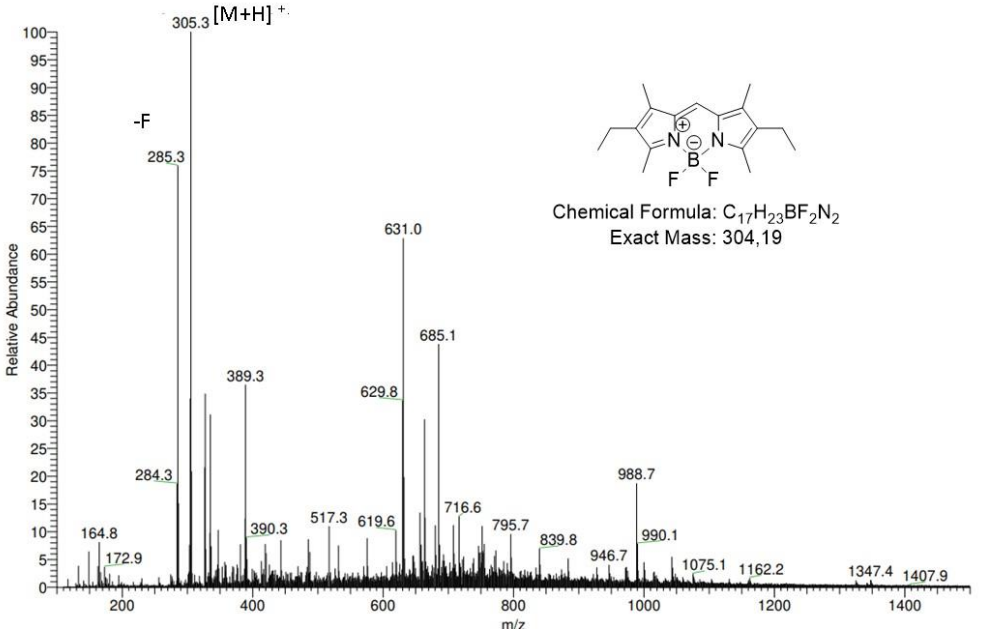

Figure 14 - Mass spectrum of the BODIPY core.

The MS^2 mass spectrum of the core allows observing peaks which correspond to the core in the absents of an ethyl group, or a methyl group, or a fluorine, as shown in figure 15.

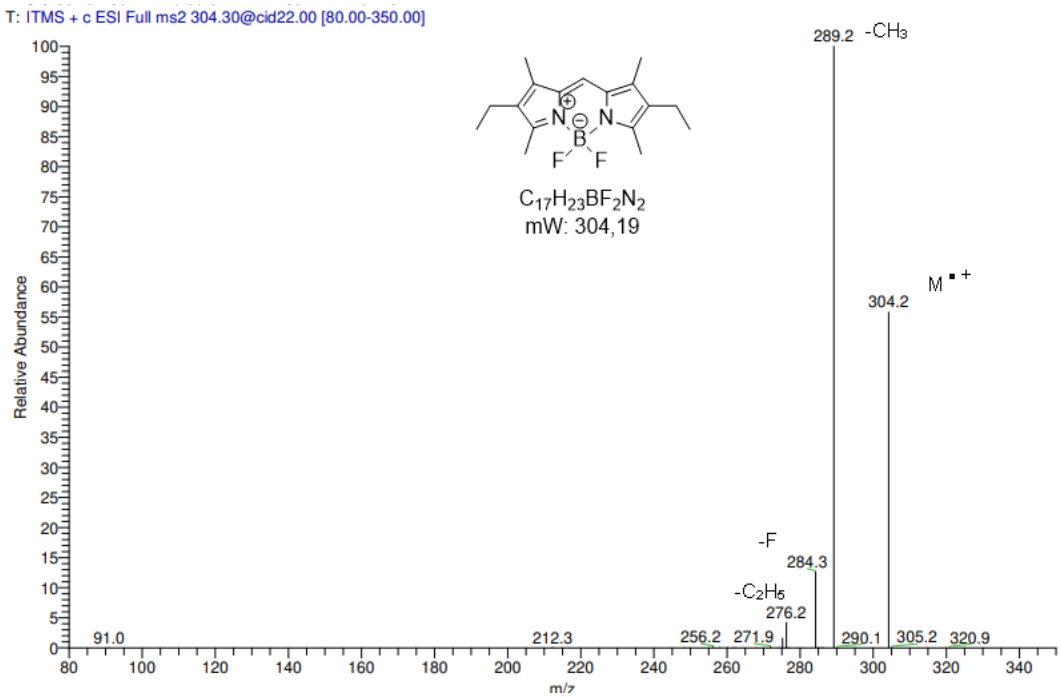

Figure 15 - ESI Full MS^2 Mass spectrum of the 304.2 ion.

In addition to completing the characterization of the two BODIPY, a FTIR analysis and comparison between the aldehyde and the product were performed, as showed in the figure 16. There is one band near 3000 cm^{-1} representing the (C-H) of the aromatic group and another near 1600 cm^{-1} representing (C =O) from the terephthaldehyde. The absence of the last band in BODIPY dimer and core shows as expected, since none of those BODIPYs have (C=O) bonds.

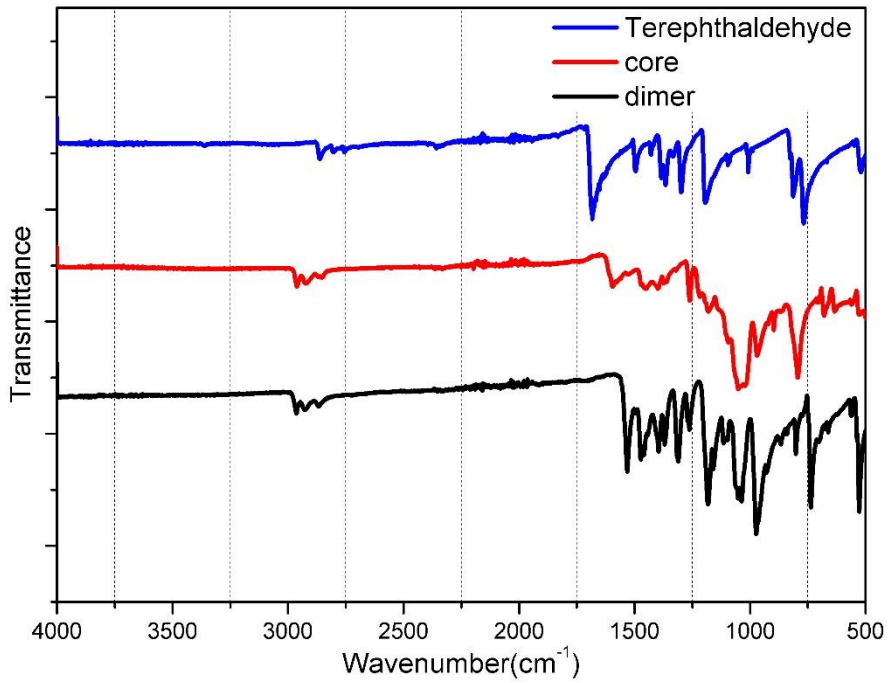

Figure 16 - Infrared ATR spectrum of terephthaldehyde, BODIPY dimer and the core.

This synthesis was repeated to guarantee reproducibility and to optimize the reaction, in terms of time and yields of the product. The final yield was 10% and the reaction was completed after 90 minutes. The reduction of the time was successful, as well as the reduction of the solvent in the reaction, and the use of a different base (triethylamine) instead of the usual (N-ethyl-diisopropylamine).

Photochemical studies of the BODIPY dimer were made, studying the absorption, emission, and excitation behaviour of the compound in different solvents. Comparing the absorption and excitation spectra, the purity of the dimer can be observed through the spectra overlapping as verified in figures 17, 18, 19 and 20. Different solvents were used to find which solvent would be more adequate for the studies. In terms of solubility, toluene was the best solvent.

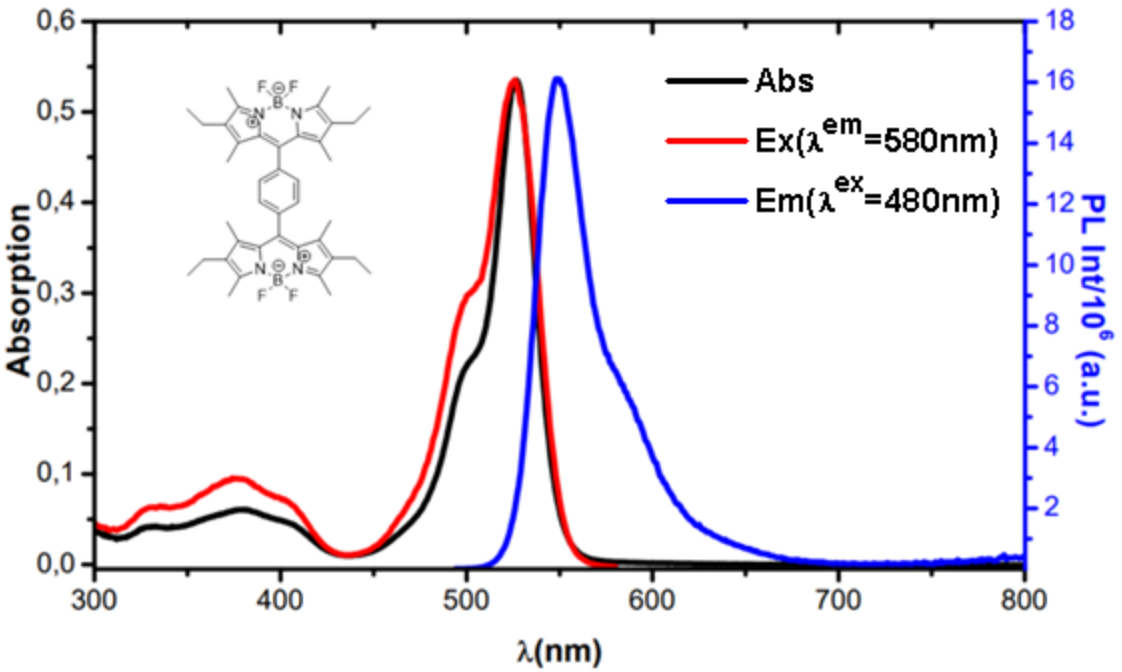

Figure 17- Absorption, emission, and excitation spectra of the dimer in toluene.

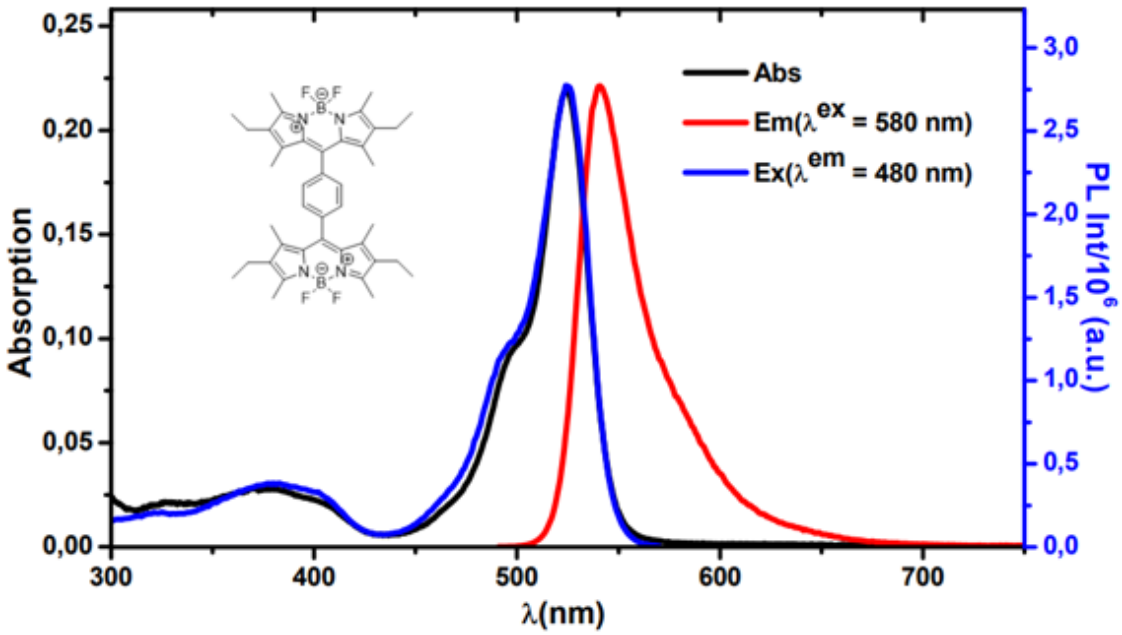

Figure 18- Absorption, emission, and excitation spectra of the dimer in ACN.

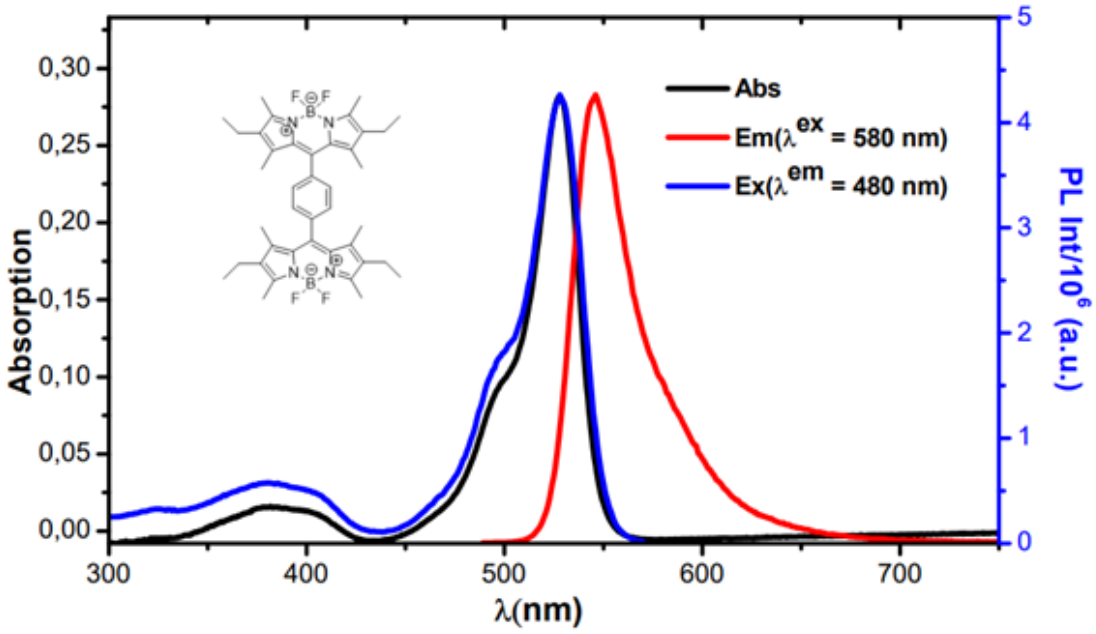

Figure 19- Absorption, emission, and excitation spectra of the dimer in DMSO.

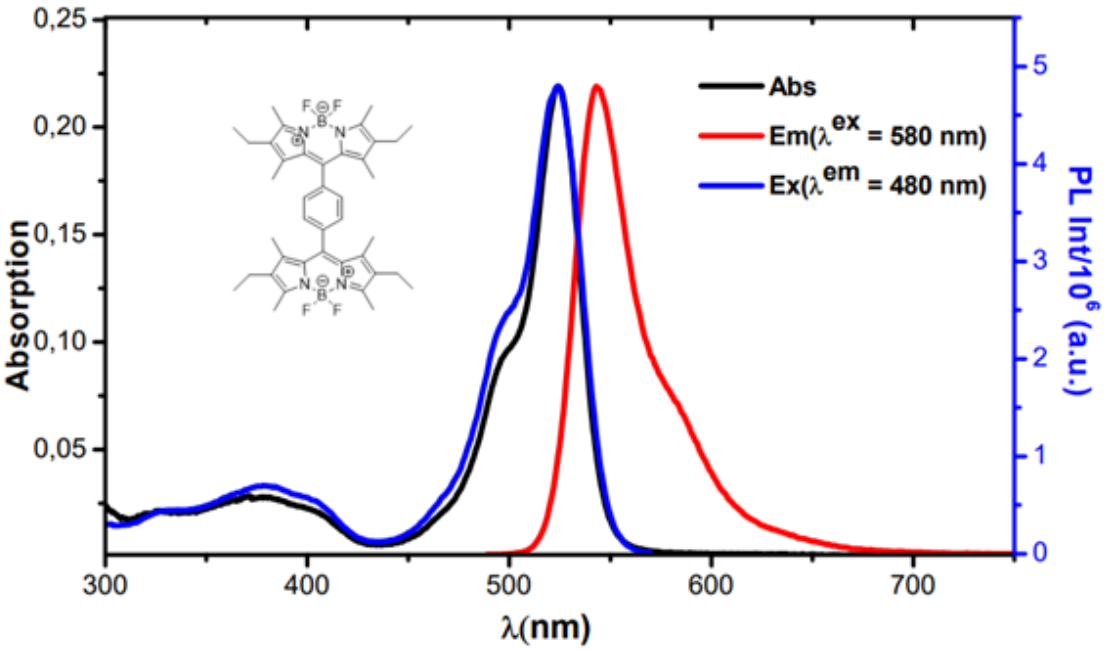

Figure 20- Absorption, emission, and excitation spectra of the dimer in THF.

Quantum yields were also calculated using the equation in figure 21, where ΦF represents fluorescence quantum yield, A_{*Em} the area of the emission spectrum, and n^{*}_{D} the refraction index. The quantum yield using the values of a molecule known in

the literature that was studied with BODIPYs (Rhodamine 6G) (Figure 22) can be calculated.

$$\Phi F = \Phi F^{P} . \frac{A^{*}_{Em}}{A^{P}_{Em}} . (\frac{n^{*}_{D}}{n^{P}_{D}})$$

Figure 21- Quantum yield equation.

In this way, the final fluorescence quantum yield of the dimer was calculated through the average of the three different values obtained, indicating a value of 67.4%

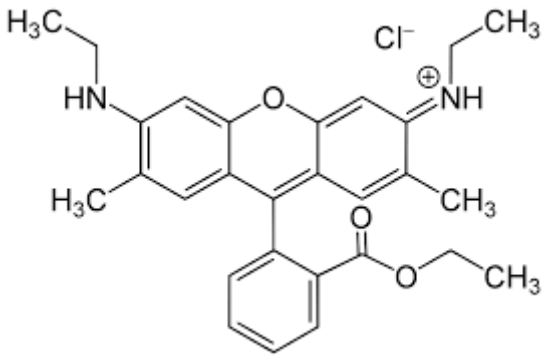

Figure 22- Chemical structure of Rhodamine 6G.

3.1.2 Synthesis of BODIPY dimer using THF

All synthesis led to the formation of a BODIPY dimer and its subproduct. The reason for this is due to the nucleophilic attack of the pyrrole to dichloromethane. Chlorine is a good leaving group, facilitating the substitution and forming a BODIPY by the attack occurring twice.[23] The next step will be testing a new synthesis, replacing the solvent with another which prevents the formation of the core.

As mentioned above, the BODIPY core is a subproduct formed by the nucleophilic attack of the pyrrole to dichloromethane. Therefore, tetrahydrofuran was used to replace the dichloromethane and thereby observe the differences between these syntheses. The synthesis of the BODIPY dimer is presented in the scheme 3.

After purification to remove impurities, a pure BODIPY dimer was obtained and was compared by TLC with one synthesized in dichloromethane, as shown in figure 23.

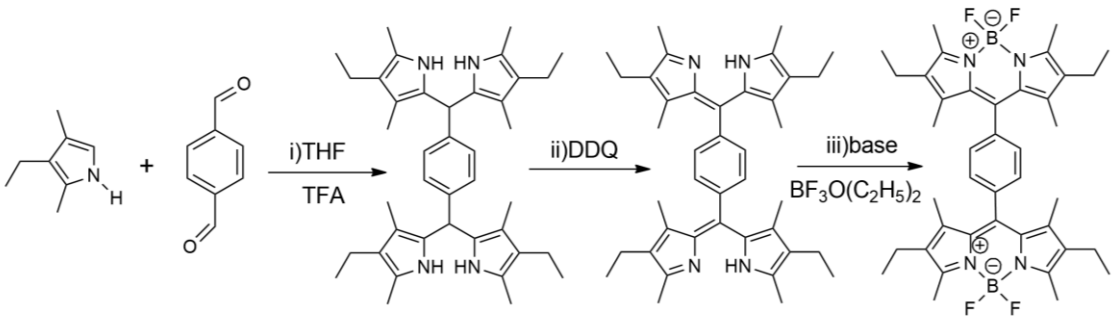

Scheme 3 - Synthesis of the BODIPY dimer using THF.

This change of solvent allowed for obtaining a purest product, which was verified during the procedure through TLC. In the figure 23, the three spots refer to BODIPY dimer synthesized in THF, DCM, and a mixture of the two samples, respectively.

Figure 23- TLC of the dimer formed by THF, DCM and the mixture of both.

Analysing figure 24 where is exhibited the absorption spectra of both products, it is noted both have the characteristic BODIPY-shaped spectra, with a maximum wavelength of 525 nm. For this reason, the two seem to be the same compound. However, a characterization by NMR will be proved the structure of the molecule.

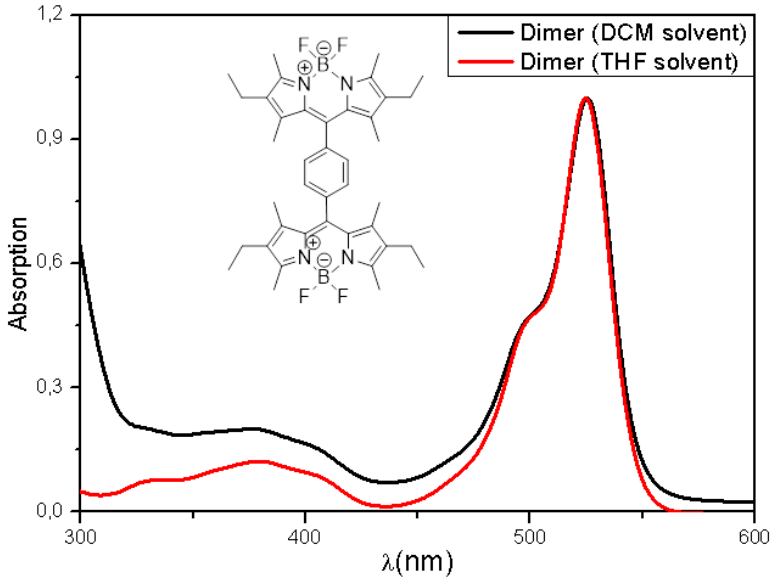

Figure 24- Normalized absorption spectra of the BODIPY dimer.

The protonic NMR analysis of the sample allowed us to identify the five peaks, which are described in figure 25 and that correspond to the hydrogens of the BODIPY dimer. Comparing the NMR spectra, there are similarities between spectra with equal peaks values and integration. This data proves the synthesis using THF as the solvent, leads to the formation of only one product, the BODIPY dimer.

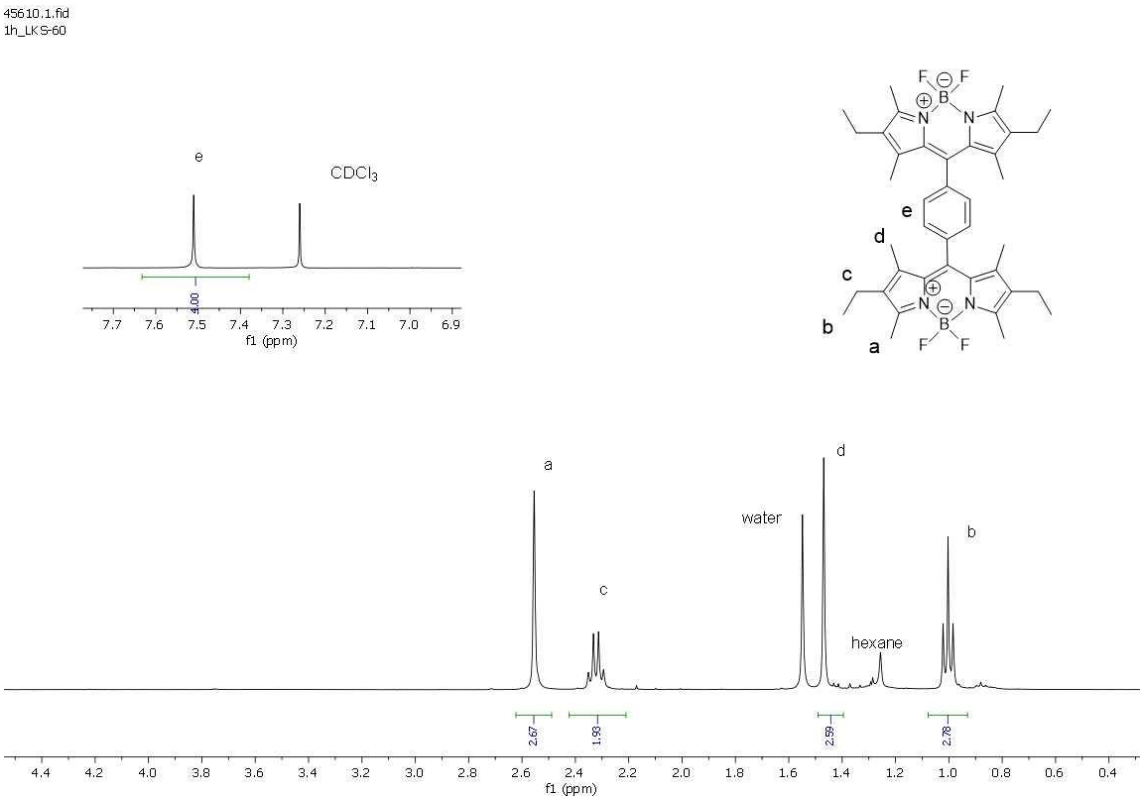

Figure 25- ^{1}H NMR of the BODIPY dimer synthesized in THF.

^{1}H NMR (400 MHz, $CDCl_3$) δ (ppm): 6.94 (s; 1H); 2.49 (s, 6H), 2.38 (q, J = 7.6 Hz, 4H), 1.48 (s, 12H), 1.00 (t, J = 7.6 Hz, 12H)

Figure 26 demonstrates the ^{13}C NMR spectrum of the BODIPY dimer. The spectrum does not have very good quality, and the most obvious explanation may be due to the low concentration of the compound. The main peaks to notice are between 12 and 18 ppm representing the two methyl and one ethyl group in the pyrrole ring, giving a total of four peaks. The carbons in the aromatic ring and pyrrole ring are represented between 130 and 155 ppm.

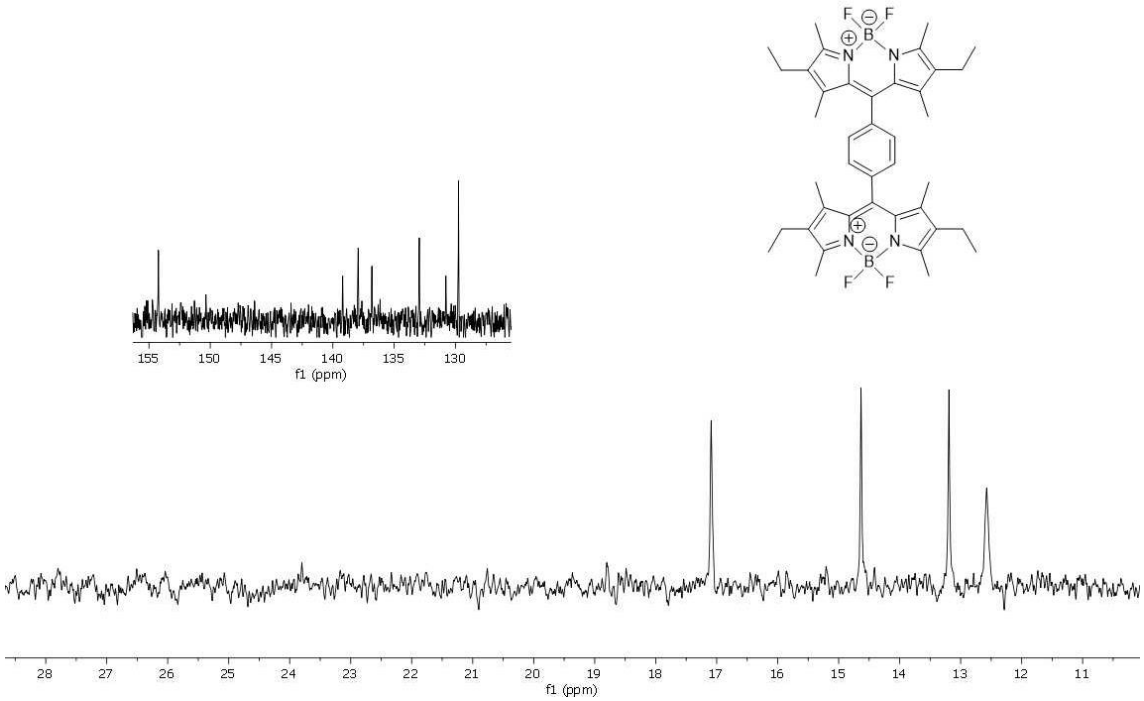

Figure 26- ^{13}C NMR of the BODIPY dimer synthetised in THF.

^{13}C NMR (100 MHz, $CDCl_3$): 153.68; 138.42; 136.81; 132.97; 129.01; 17.12; 14.61; 13.27; 12.64

Fluorine having just one natural isotope, Fluorine-19, has a nuclear spin, I, of ½. Boron has a natural abundance of 19.9% of ^{10}B which has a nuclear spin of 3 and ^{11}B has a natural abundance of 80.1% with a nuclear spin of 3/2. Thus, the spectrum observed will be mainly prevailed by ^{11}B NMR. The fluorine is coupled with boron in a fluorine-boron (^{11}B-^{19}F) bond, using the 2nI+1 rule, and as n is the number of boron nuclei (n=1), this coupling should result in four peaks with equal intensities (1:1:1:1) as shown in Figure 27.

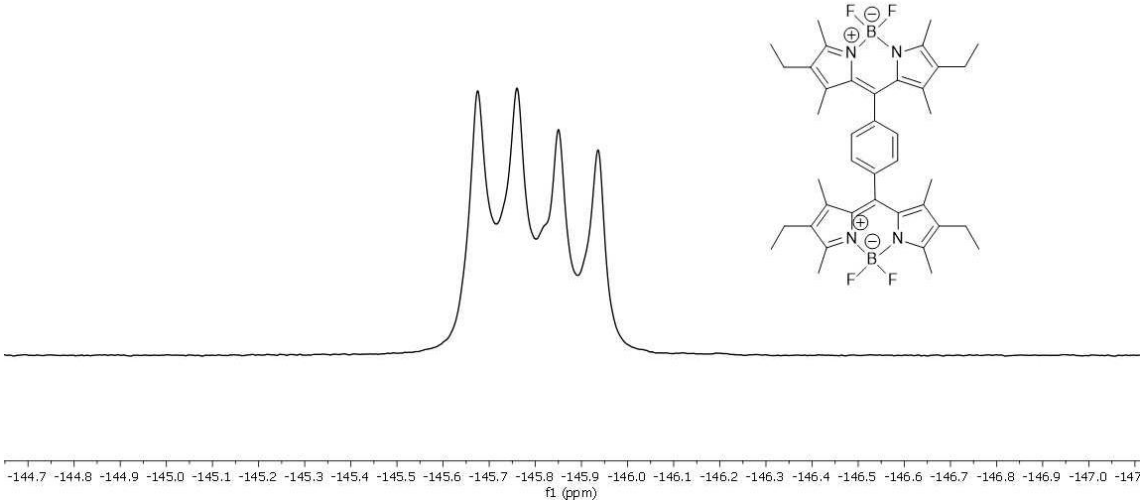

Figure 27- ^{19}F NMR of the BODIPY dimer synthesized in THF.

^{19}F NMR (376 MHz, $CDCl_3$) δ (ppm): -145.80 (q, J = 33.46 Hz, 4F)

Boron has two naturally occurring NMR active nuclei. Both nuclei have spins of greater than ½ and are quadrupolar. ^{11}B has a spin of 3/2 and ^{10}B is a spin of 3. ^{11}B nucleus is the more representative and therefore will show a triplet by coupling with the two fluorine atoms.

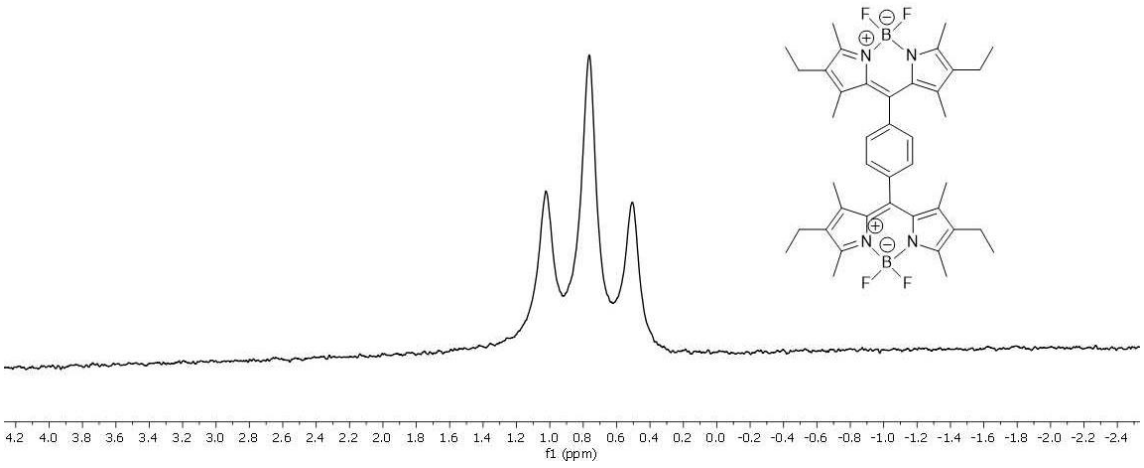

Figure 28- ^{11}B NMR of the BODIPY dimer synthesized in THF.

^{11}B NMR (128 MHz, $CDCl_3$) δ (ppm): 0.77 (t, J = 33.28 Hz)

In sum, both syntheses already presented lead to the formation of BODIPY dimer. However, the replacement of DCM with THF improved the yield, from 10% to 17%. The fact that the core is not formed, and the purification process is easier, increases the yield that shows as an advantage for this type of reactions.

3.1.3 Synthesis of Meso-Phenyl BODIPY (BODIPY 3)

The synthesis of Meso-Phenyl BODIPY was intended to serve as a comparison to the BODIPY dimer, in terms of chemical characterization and biological studies. The scheme 4 shows the reaction conditions of the experimental procedure.

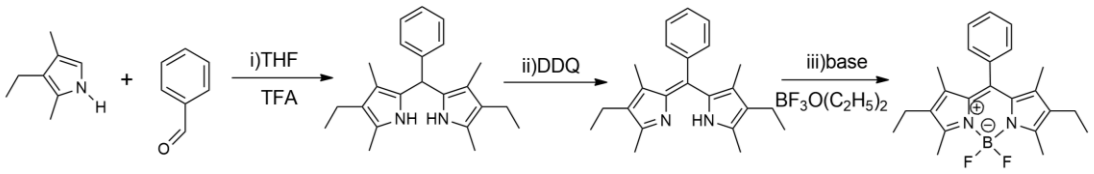

Scheme 4 – Synthesis of Meso-Phenyl-BODIPY.

The protonic NMR spectrum (figure 29) contains residues of water and chloroform at 1.56 ppm and 7.26 ppm, respectively.[47] The phenyl group has three different hydrogens, but the *meta* and *para* protons are very similar and therefore represent a triplet, and in the *ortho* position a duplet at about 7.3 and 7.47 ppm in the aromatic zone. A triplet at 0.98 ppm and a quartet at 2.3 ppm are shown which represents an ethyl group. Finally, two singlets at 1.27 and 2.53 ppm represent two methyl groups.

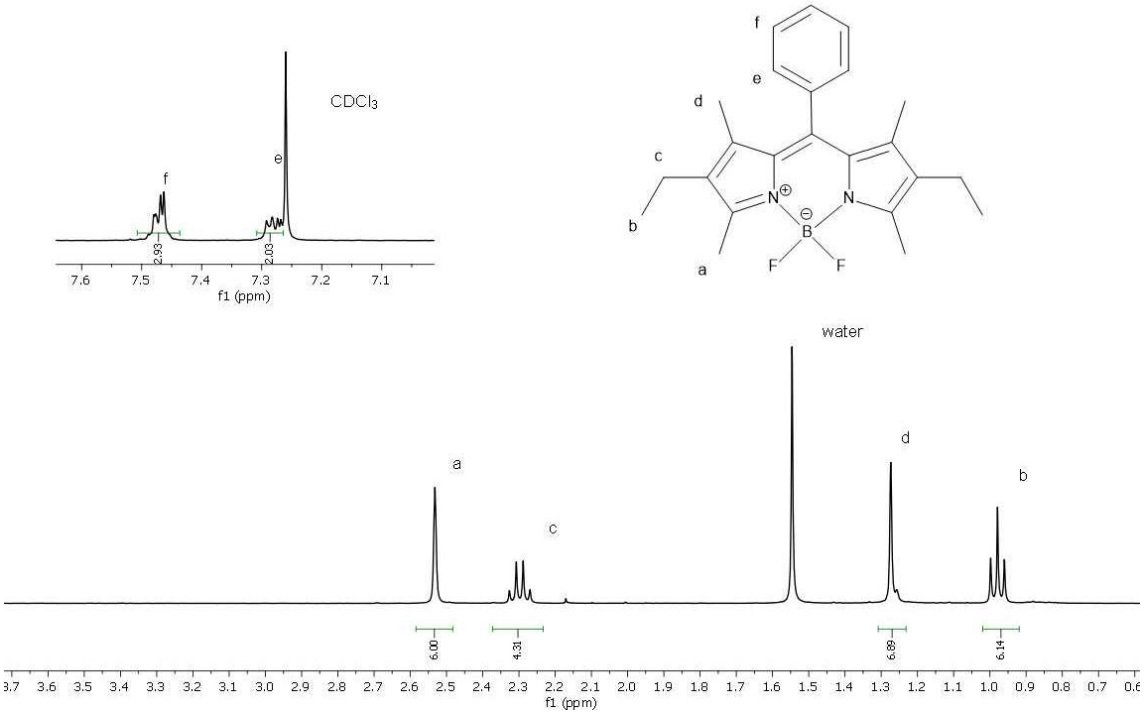

Figure 29 - ^{1}H NMR spectrum of Meso-Phenyl-BODIPY.

After identification of Meso-Phenyl BODIPY in protonic NMR, we proceeded to the characterization by ^{13}C, ^{19}F, and ^{11}B NMR. Figure 30 (A) is presented ^{13}C NMR where the peaks corresponding to carbons were identified. As expected in ^{19}F NMR, there are four peaks with equal intensities (1:1:1:1), which are a result of the coupling between fluorine and boron (figure 30 (B)). The ^{11}B NMR spectrum (figure 30 (C)) shows that there is a boron-type molecule indicating the presence of a BODIPY.

(A)

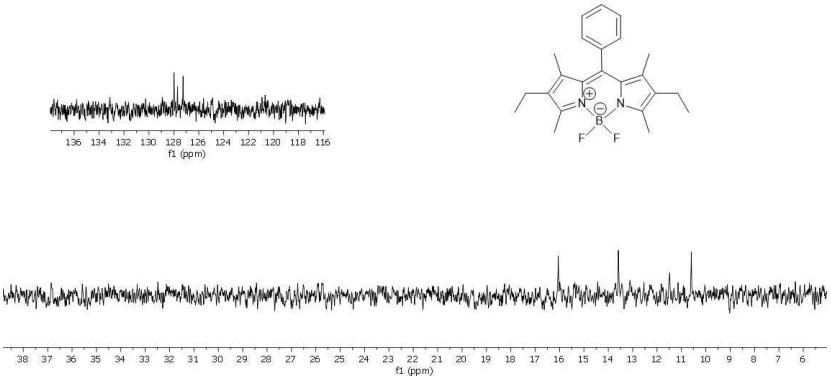

^{13}C NMR (100 MHz, $CDCl_3$): 128.14; 127.90; 127.34; 16.21; 13.73; 10.68

(B)

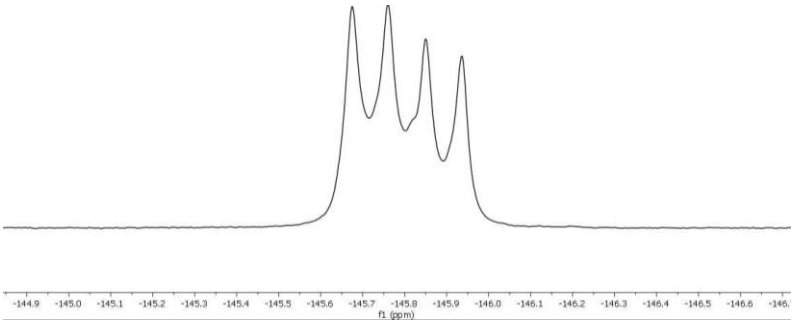

^{19}F NMR (376 MHz, $CDCl_3$) δ (ppm): -145.80 (q, J = 33.46 Hz, 2F).

(C)

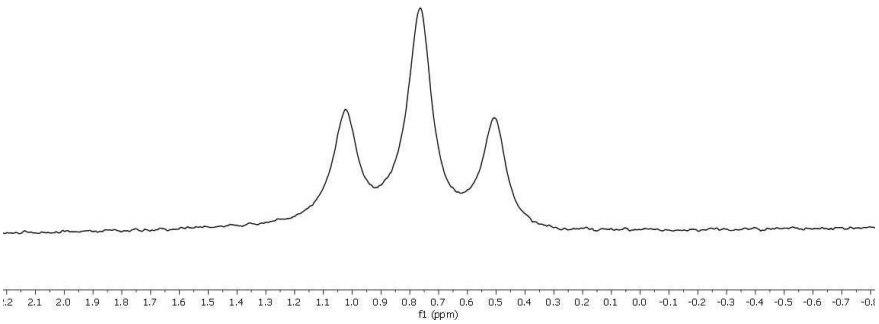

^{11}B NMR (128 MHz, $CDCl_3$) δ (ppm): 0.80 (t, J = 33.28 Hz).

Figure 30 - (A) " ^{13}C NMR spectrum of Meso-Phenyl-BODIPY" ; (B) " ^{19}F NMR spectrum of Meso-Phenyl-BODIPY" and " ^{11}B NMR spectrum of Meso-Phenyl-BODIPY".

The analysis of the mass spectrum of Meso-Phenyl-BODIPY made possible the identification of the molecular ion at 381.4 m/z and a big abundance of the fragmentation of a fluorine group (figure 31).

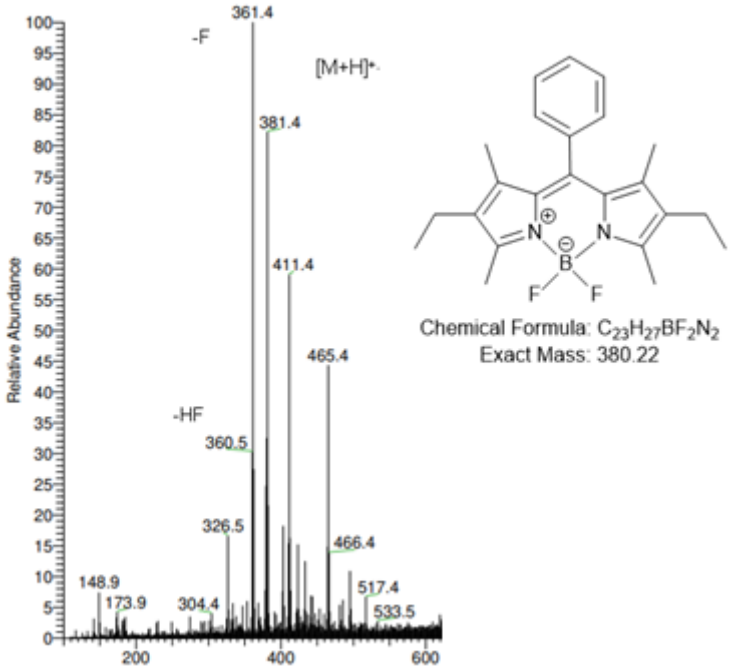

Figure 31 - Mass spectrum of Meso-Phenyl-BODIPY.

As MS^2 spectrum is more specific and analyses only the mass of the BODIPY compound, showing more typical fragmentations, methyl, and ethyl groups with a ratio of 366.3 m/z and 353.3 m/z were detected.

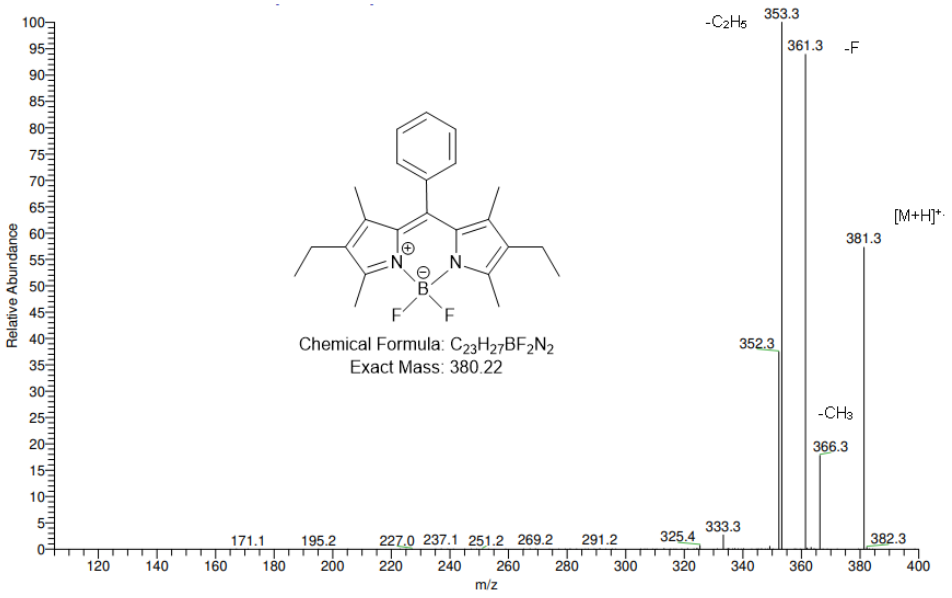

Figure 32 - MS^2 mass spectrum of the fragment 381.3 m /z.

In terms of the light absorption spectrum of Meso-Phenyl-BODIPY (figure 33 A) shows a strong band very characteristic of BODIPY compounds at 525.3 nm with a weak band in the ultraviolet zone at 375 nm.

The main reason of the FTIR-ATR spectrum is to see if there is some type of oxygen or nitrogen vibration type band, and characteristic bands until 1500 cm^{-1} are identified (figure 33 B).

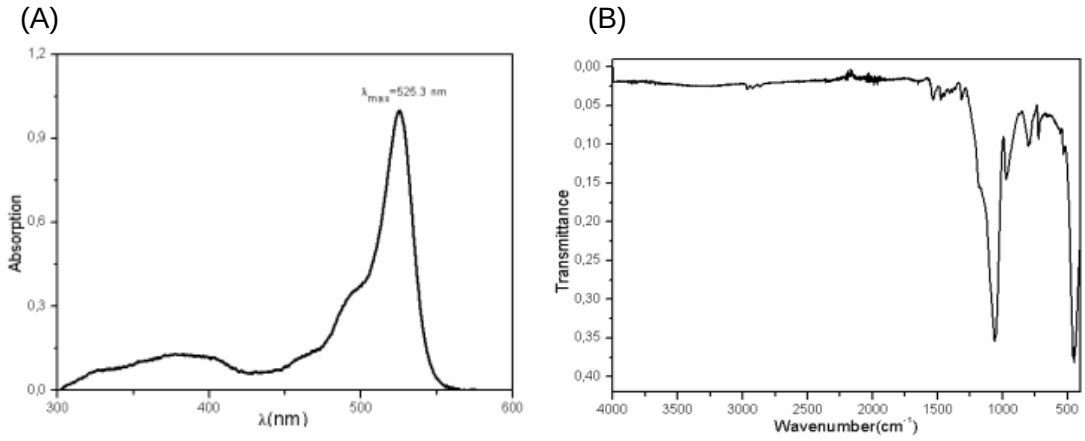

Figure 33- Absorption spectrum (A) and ATR spectrum (B) of the Meso-Phenyl-BODIPY.

We analysed the photochemical studies involving the absorption, emission, and excitation spectra of the Meso-Phenyl BODIPY. All the spectra corresponded to the BODIPY-type bands, and the overlap of the absorption and excitation showed the purity of the compound. The quantum yield of fluorescence was calculated and compared with Rhodamine 6G. The result was 56.4% fluorescence quantum yield.

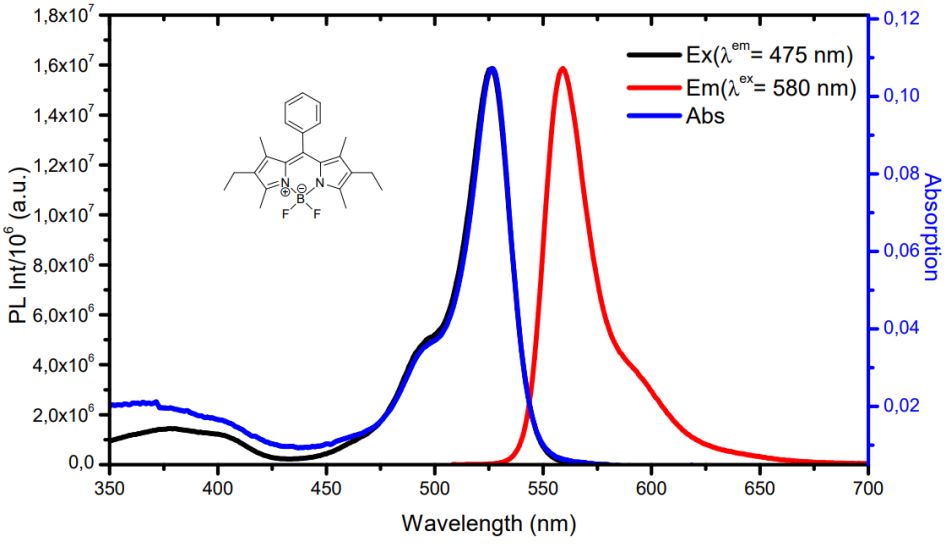

Figure 34- Absorption, emission, and excitation spectra of Meso-Phenyl-BODIPY.

3.1.4 Synthesis of BODIPY Trimer (BODIPY 4)

The objective was to synthetise a new compound with three BODIPY units and compared with the other aromatic BODIPYs synthesized. The next scheme 5 is presented the reaction to form the pretended product.

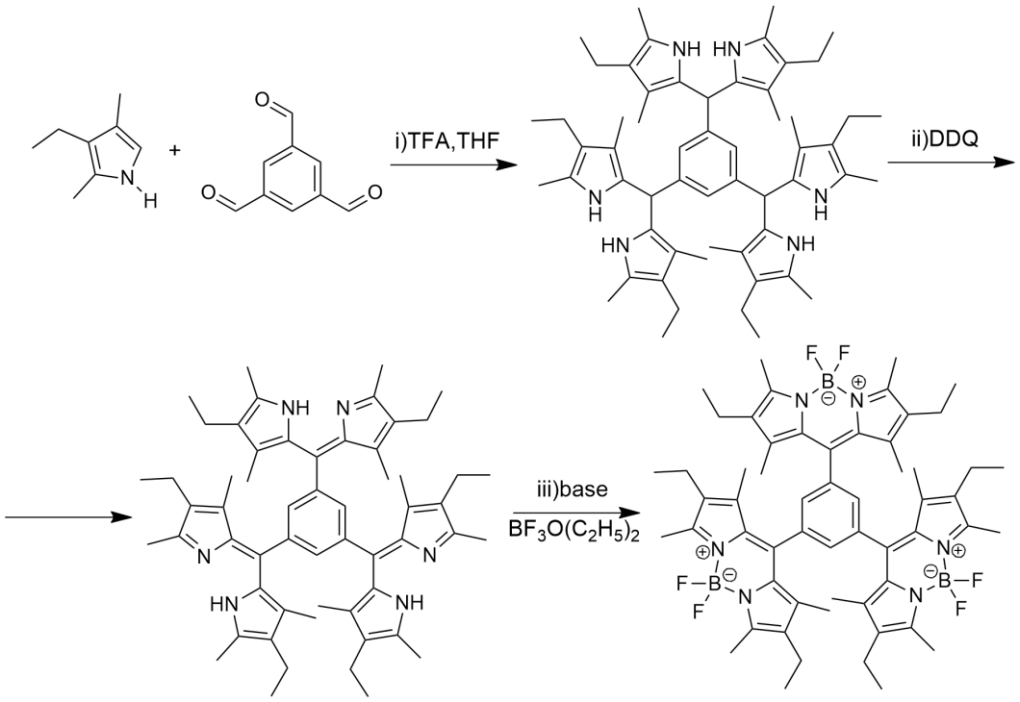

Scheme 5- Synthesis of the BODIPY trimer.

After purification, five different compounds were isolated. The first fraction was a light blue colour solution in low quantity, that we supposed corresponding to the non-oxidized dipyrromethane. The second and third fraction were strong yellow colour, the fourth a red and which by amount seems to be the BODIPY trimer and the firth fraction was dark red. All compounds corresponded to different molecules, as shown in absorption spectra in figure 35. They have a different absorption maximum, although their values are close.

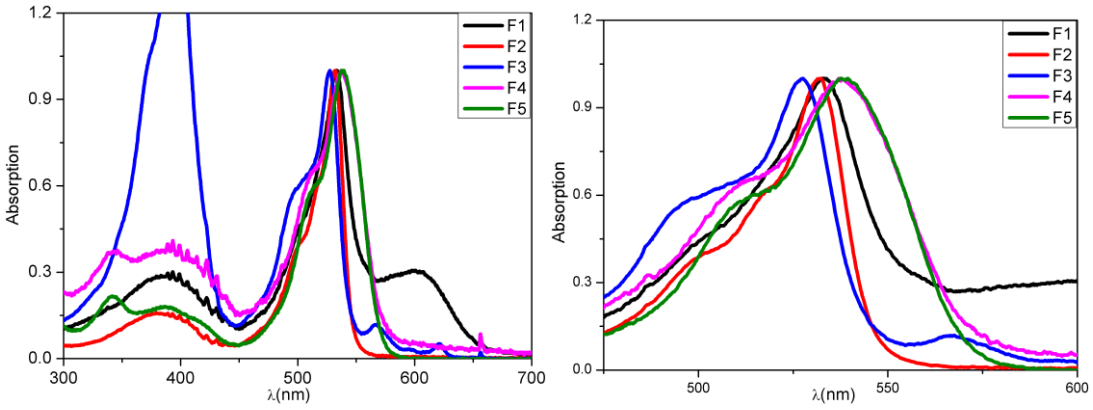

Figure 35- Absorption spectraof all 5 fractions formed in the BODIPY trimer reaction.

Only two of the five fractions had enough amount to proceed the characterization. One of them was the F2 which had a characteristic BODIPY-type UV-Vis spectrum, with a maximum wavelength of 532 nm (figure 36).

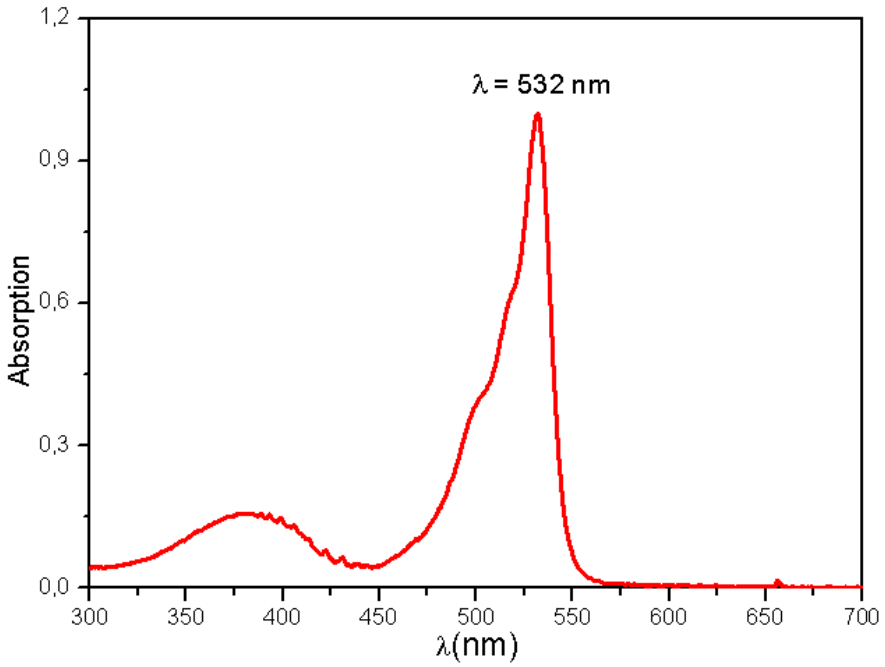

Figure 36- UV-vis spectrum of the F2 compound.

The full mass spectrum of F2 showed that the most abundant compound is at 749.9 m/z., as shown in figure 37. However, this molecular mass do not correspond to the BODIPY trimer. Possibly, the molecule can be another BODIPY formed during the process, as shown in figure 37 the mass corresponds to an incomplete trimer BODIPY, where the remaining carboxyl group was oxidized to a carboxylic acid.

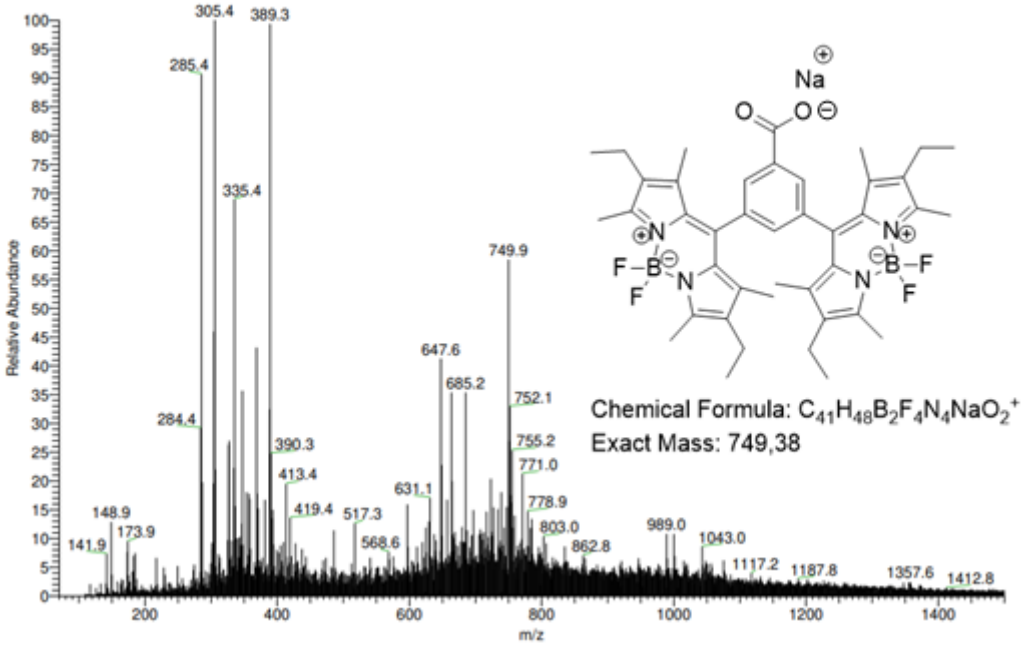

Figure 37- Mass spectrum of the fraction F2.

In fact, analysing the MS^2 spectrum of the fragment 750 m/z indicates the molecule has two BODIPY units and a carboxaldehyde acid, the last was result of the oxidation of the aldehyde, in the structure. Even the 750 m/z fragment, a sodium ion could be near to the acid group. This information leads to the molecule presented in figure 38.

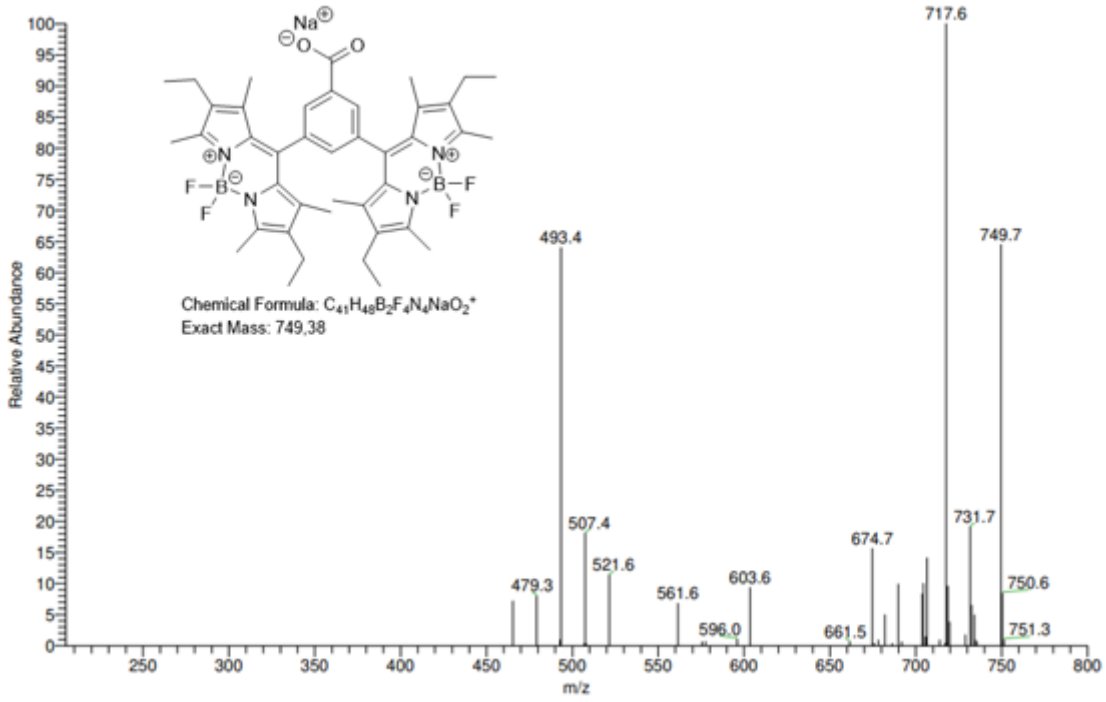

Figure 38- MS^2 spectrum of the fraction F2.

Figure 39 presents the protonic NMR of the COOH-dimer-BDP, the second fraction of the trimer reaction.

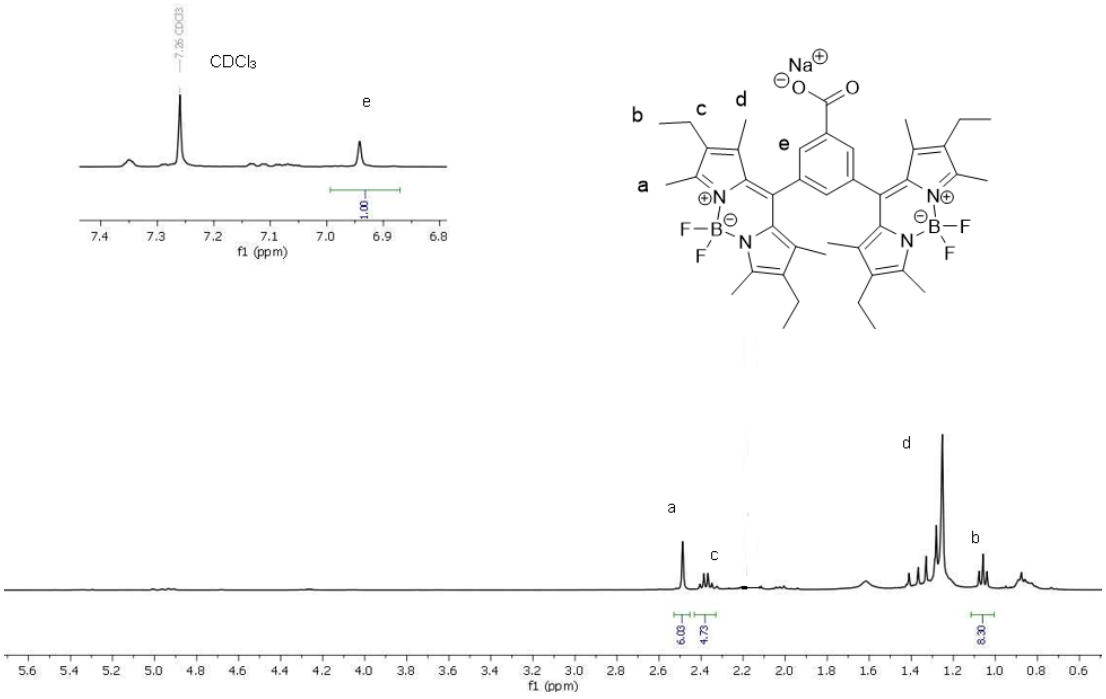

Figure 39- ^1H NMR spectrum of fraction F2.

Another compound characterized was the fourth fraction. In figure 40, the full mass spectrum of the compound allowed the identification of BODIPY trimer through the peak at 985.7.

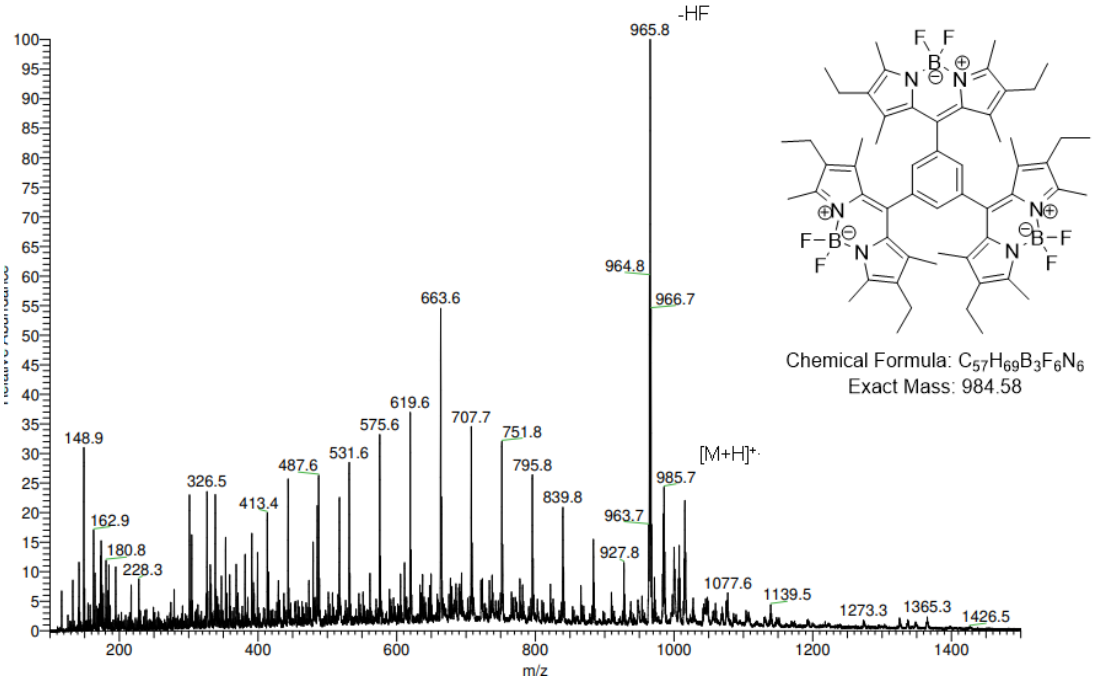

Figure 40- Full MS spectrum of the BODIPY trimer.

The MS^2 spectrum revealed the exact mass of the trimer as well as, intense peaks that correspond to the fragmentation of methyl group at 970.7 m/z, a fluorine at 965.7 m/z and an ethyl group at 956.6 m/z. These fragmentations are the more common fragmentations in BODIPY-type molecules (figure 41).

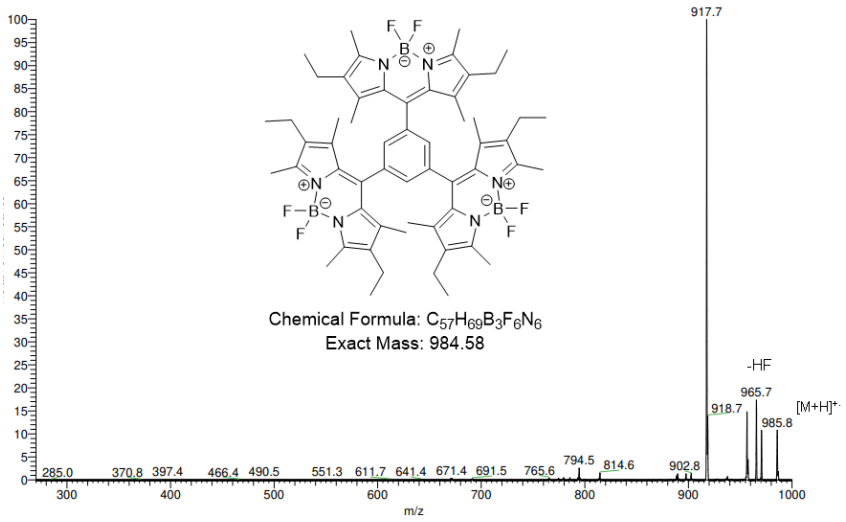

Figure 41- MS^2 of the BODIPY trimer.

In the ^{1}H NMR spectrum (figure 42), a triplet and a quartet at 1.01 and 2.31 ppm, correspond the ethyl group and two singlets at 1.69 and 2.54 ppm to the methyl groups of the BODIPY. There is also a peak at 7.74 ppm, in the aromatic zone, defined by the three protons at the phenyl in the centre of the molecule.

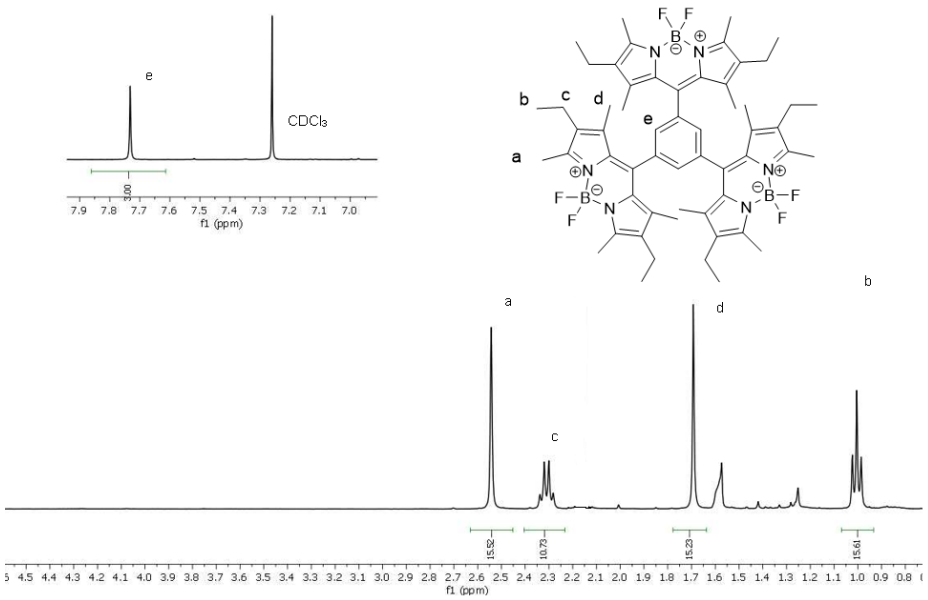

Figure 42- ^{1}H NMR of the BODIPY trimer.

^{1}H NMR (400 MHz, $CDCl_3$) δ (ppm): 7.74 (s; 3H); 2.54 (s, 18H), 2.31 (q, J = 7.6 Hz, 12H), 1.69 (s, 18H), 1.01 (t, J = 7.6 Hz, 18H)

The synthesis was repeated, changing some conditions to optimize the process. The reaction was heated in a water bath at 40°C for 90 minutes. This increase in time was because 30 minutes could not be enough to make all the pyrrole attacks. The fact of BODIPY molecules are close to each other, can promote some steric hindrance, making more difficult the reaction and formation of the third BODIPY unit. The result was better than the previous reaction, decreasing the number of subproducts and impurities.

3.1.5- Preliminary studies in the bromination of the BODIPY dimer

NBS (N-bromo succinimide) is a gleaming white crystalline solid and easy to work with. It will do many of the same reactions as bromine where this molecule has attached to the electron-withdrawing nitrogen of succinimide, the bromine, that has a partial positive charge and is therefore electrophilic.

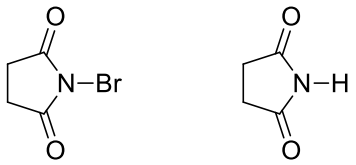

Figure 43 - Molecular structure of N-bromo succinimide and succinimide.

Allylic bromination is the replacement of a hydrogen on a carbon adjacent to a double bond, or in the case of an aromatic ring, designated as benzylic bromination. NBS is used as a substitute for Br_2 in these cases, since Br_2 tends to react with double bonds to form dibromides. The advantage of NBS is that provides a low-level concentration of Br_2 in reaction, and bromination of the double bond doesn't compete as much.

Once Br_2 is formed, the reaction proceeds like other free-radical halogenation reactions. First, homolytic cleavage of the Br_2 with light or heat initiates the reaction, followed by the abstraction of the allylic H. Then, the reaction of this radical with another equivalent of Br_2 occurs to give the desired product. The remaining Br radical reacts again with another equivalent of the hydrocarbon in this chain reaction, until the limiting reagent is consumed.

The objective of this reaction was to see if occurs bromination and where could it occur in the BODIPY dimer. The synthesis consisted of the addition of dimer and NBS (1:1) stoichiometry with an increment of 10% of NBS at room temperature and pressure for 72 hours. The reaction mixture had two phases with different colours, one was lighter red and another dark red. Both phases were analysed by TLC and absorption spectra, as shown in figure 44. Analysing the absorption behaviour of the product, it is possible to verify that the spectra are maintained over time, indicating that the reaction did not occur.

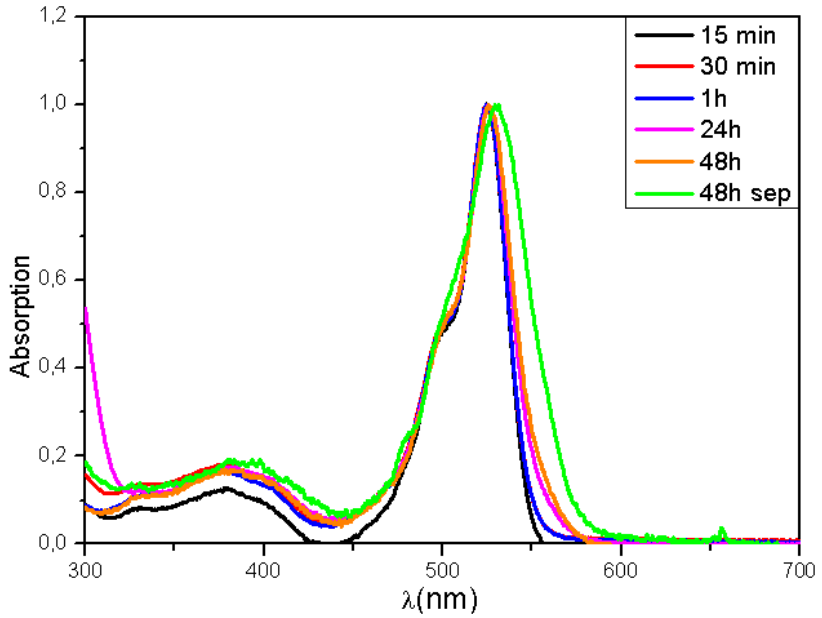

Figure 44- Absorption spectra of the bromination of the dimer.

A new attempt using a different BODIPY, in this case Meso-Phenyl-BODIPY, was tried, maintaining the same reaction conditions for 48 hours. The reaction was controlled by the UV-Vis spectroscopy over time. The final product was compared with Meso-Phenyl-BODIPY and Bromo-Phenyl-BODIPY, the last already synthesized in another lab work, as shown in figure 45. All three spectra have BODIPY-like bands, Meso- Phenyl-BODIPY has a maximum wavelength of 525 nm and with the bromine, there is a Shift to 528 nm. After 48h of reaction, the product of the bromination showed a spectrum with the same wavelength of the Bromo-Phenyl-BODIPY, but with a slight difference in the shoulder of the band, which can mean that the attack of the bromine occurred in another functional group, instead of the phenyl, at least in the *para* position of the benzene.

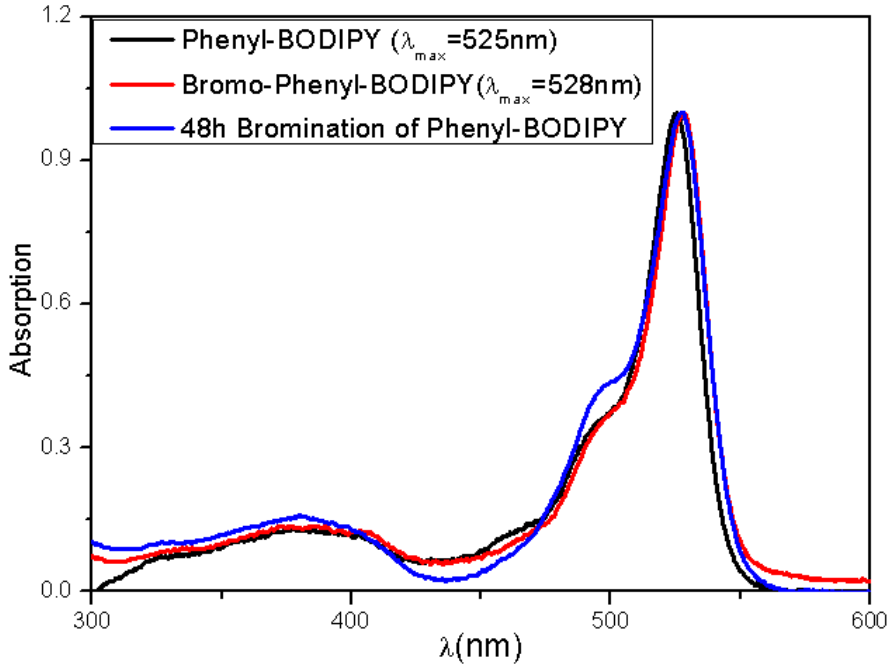

Figure 45 - UV-vis spectrum of Phenyl-BODIPY, Bromo-Phenyl-BODIPY and the product of the bromination of Phenyl-BODIPY.

Other methods of characterization would be required to find the structure of the product.

3.2 Synthesis of Aliphatic BODIPYs

The aim of this subchapter was to synthesize three BODIPYs from aliphatic aldehydes (iso-butyl aldehyde and acetaldehyde) and characterize by NMR, absorption spectroscopy and mass spectrometry. A comparison between the synthesis involving between aromatic and aliphatic aldehydes will be discussed.

3.2.1 Synthesis of Meso-Iso-Propyl-BODIPY

The next scheme 6 showed the condition reaction followed in the synthesis. The Meso-Iso-Propyl-BODIPY had a yield of 4%.

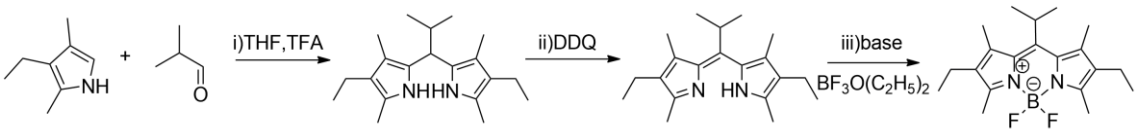

Scheme 6- Synthesis of iso-propyl-BODIPY.

After purification, three products were obtained and characterized by absorption spectroscopy. In figure 46, the graph has BODIPY similarities spectra with two bands. The main band with a maximum wavelength near 530 nm with a shoulder and a second near 350 nm.

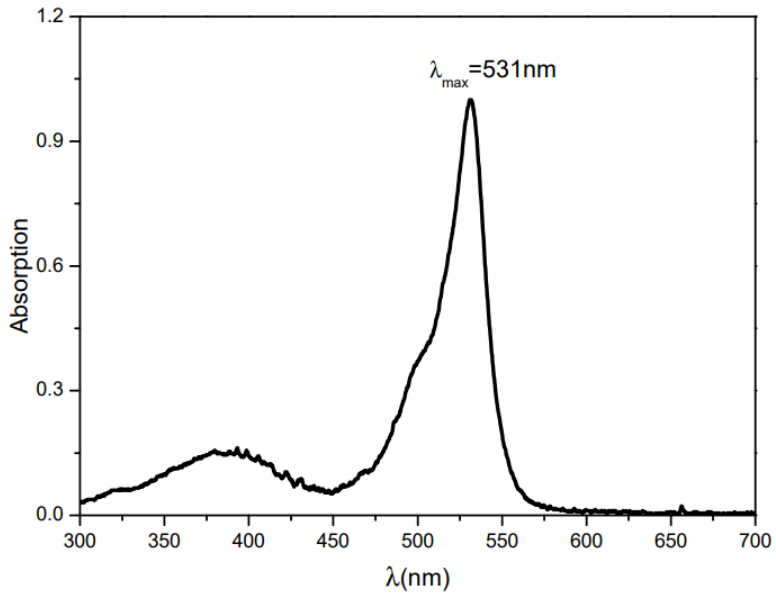

Figure 46- Normalised absorption spectrum of iso-propyl-BODIPY.

The amounts of the products were low, and the chemical characterization of only one fraction was possible.

The protonic NMR shows the protons of the Meso-Iso-Propyl-BODIPY in figure 47. A triplet at 1.1 ppm, a quadruplet at 2.4 ppm, and two singlets representing the protons of the core and subsequently there is a multiplet and a duplet near 4.0 and 1.5 that represent the CH and CH_3 protons of the iso-propyl group on the meso position.

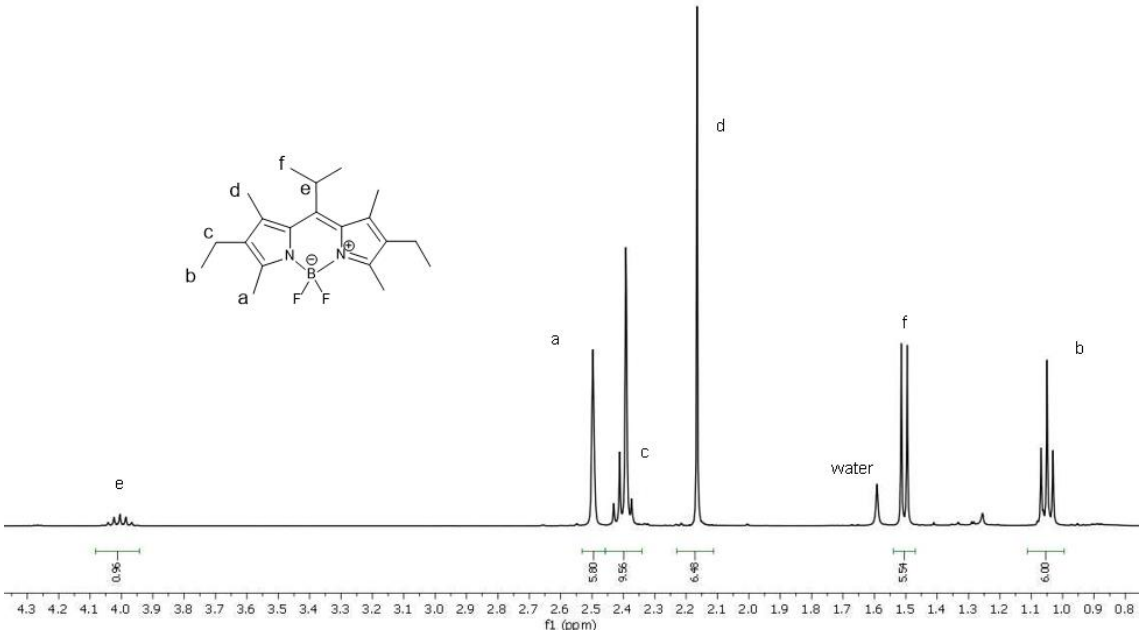

Figure 47 - ^{1}H NMR spectrum of Meso-Iso-Propyl-BODIPY.

^{1}H NMR (400 MHz, $CDCl_3$) δ (ppm): 4.02(m,1H); 2.49 (s, 6H), 2.38 (q, J = 7.6 Hz, 4H), 2.18 (s, 12H); 1.51 (d, 12H), 1.05 (t, J = 7.6 Hz, 12H)

Analysing the ^{13}C, ^{19}F and ^{11}B NMR presented in figure 48, it was possible to confirm the presence of the pretended BODIPY. However, in ^{19}F NMR, there is a small quartet which indicate the sample is not pure and can be corresponded to another BODIPY. In ^{11}B NMR, there is a triplet, as expected.

(A)

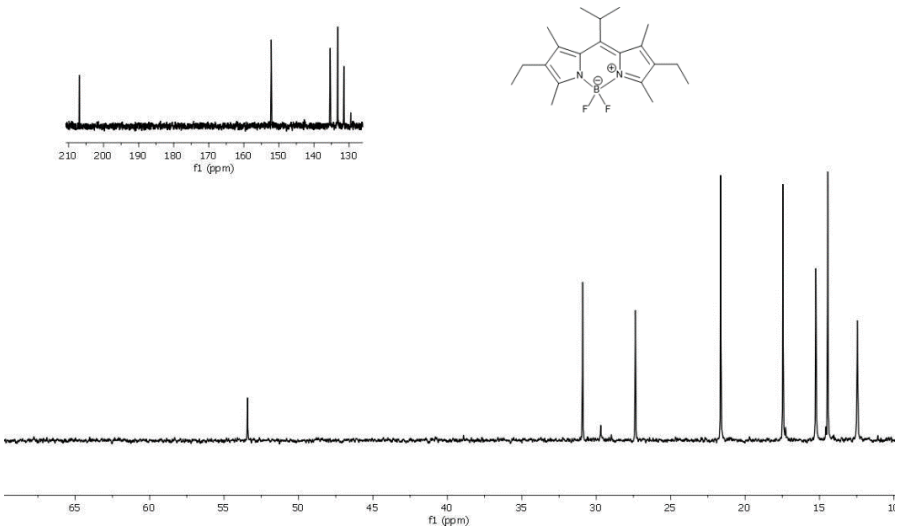

^{13}C NMR (100 MHz, $CDCl_3$): 205.95; 152.19; 135.34; 133.24; 131.48; 53.43; 30.91; 27.37; 21.64; 17.46; 15.25; 14.45; 12.46

(B)

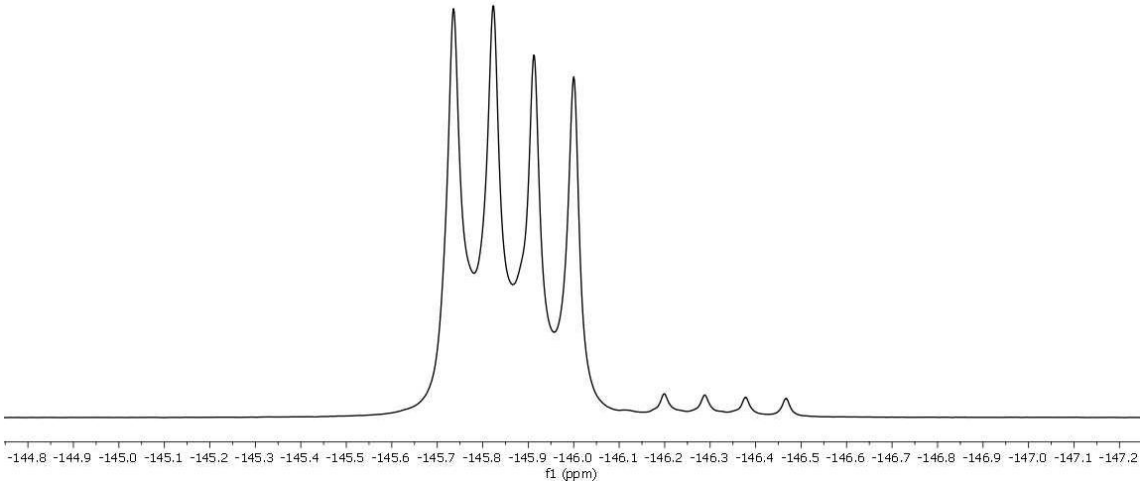

^{19}F NMR (376 MHz, $CDCl_3$) δ (ppm): -145.85 (q, J = 33.46 Hz, 2F); -146.33 (q, J = 33.46 Hz, 2F)

(C)

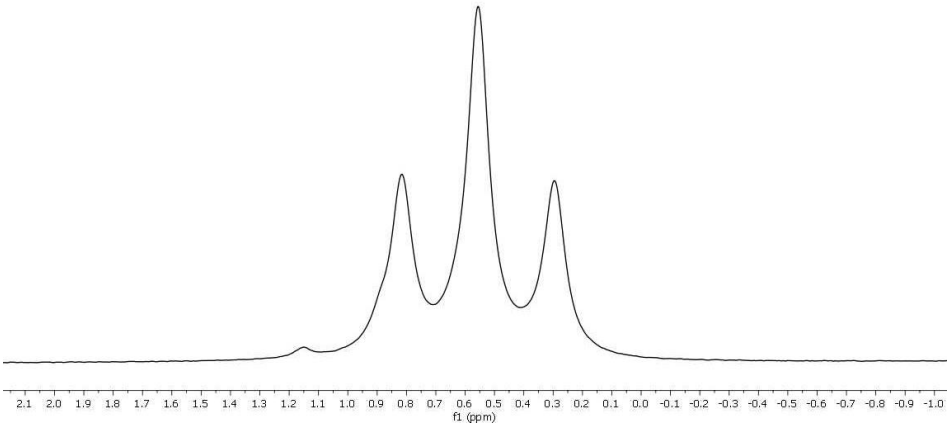

^{11}B NMR (128 MHz, $CDCl_3$) δ (ppm): 0.49 (t, J = 33.28 Hz).

Figure 48- (A) "^{13}C NMR spectrum of Meso-Iso-Propyl-BODIPY"; (B) "^{19}F NMR spectrum of Meso-Iso-Propyl-BODIPY" and (C) "^{11}B NMR spectrum of Meso-Iso-Propyl-BODIPY".

The full mass spectrum identified the BODIPY compound at 347.4 m/z, and a very characteristic peak at 327.4 m/z, symbolizing the BODIPY without the HF group (figure 49).

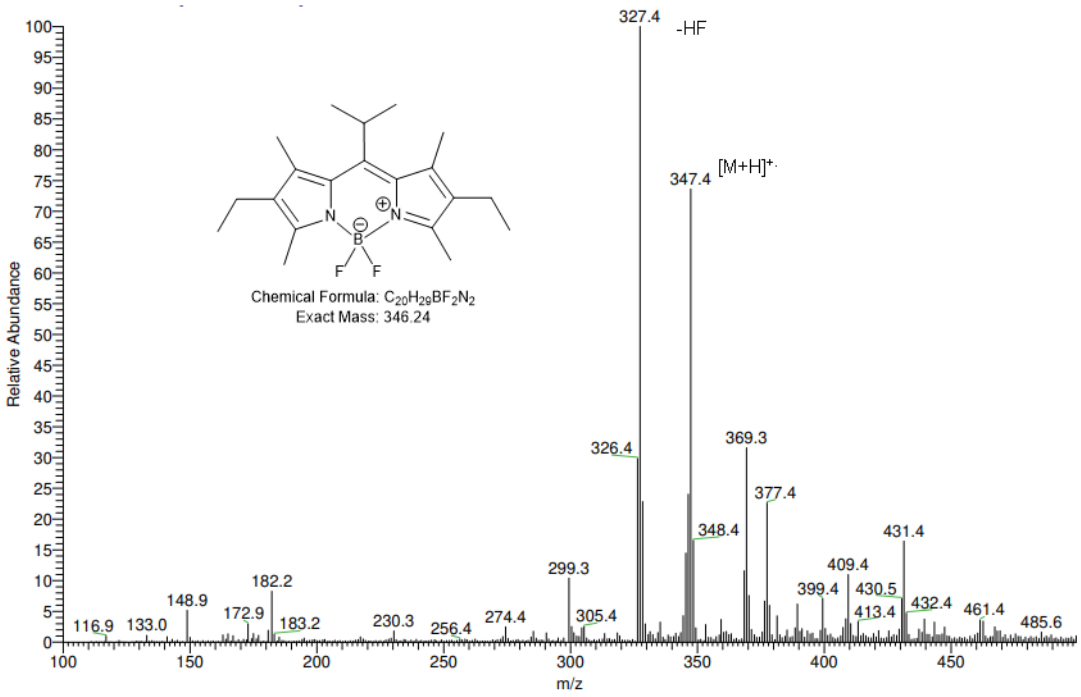

Figure 49- Mass spectrum of iso-propyl-BODIPY.

The MS^2 spectrum of the fragment 347.4 z/m presented peaks of the most obvious leaving groups, such as fluorine, methyl, and ethyl group, as shown in figure 50.

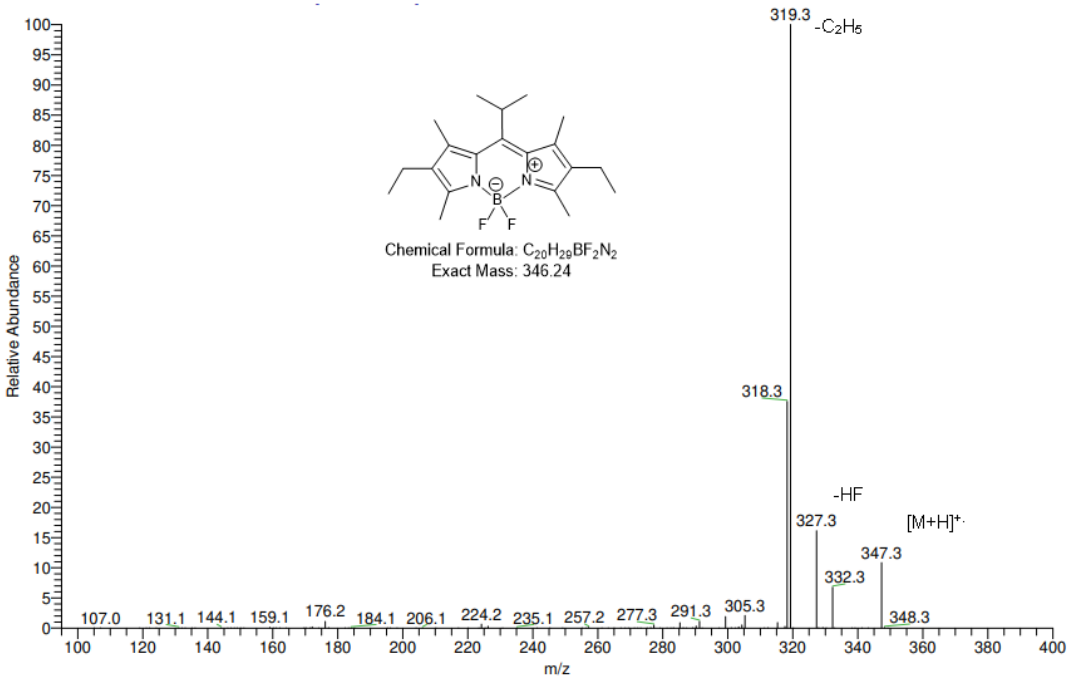

Figure 50- MS^2 of Meso-Iso-Propyl-BODIPY.

3.2.2 Synthesis of Meso-Methyl-BODIPY (BODIPY 7)

The BODIPY was obtained by following the reaction in scheme 7. The isolated product was analysed by absorption spectroscopy. In normalized absorption spectrum, a maximum wavelength at 528.7 nm can be noted, as shown in figure 51.

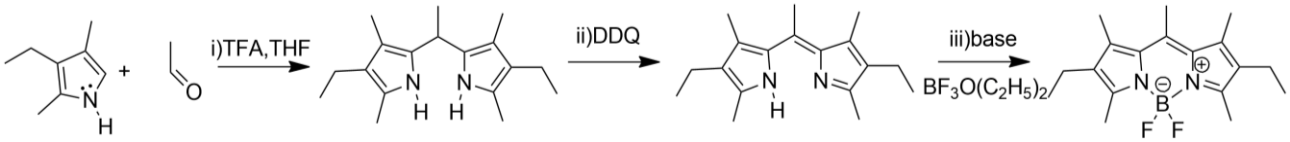

Scheme 7-Synthesis of Meso-Methyl-BODIPY.

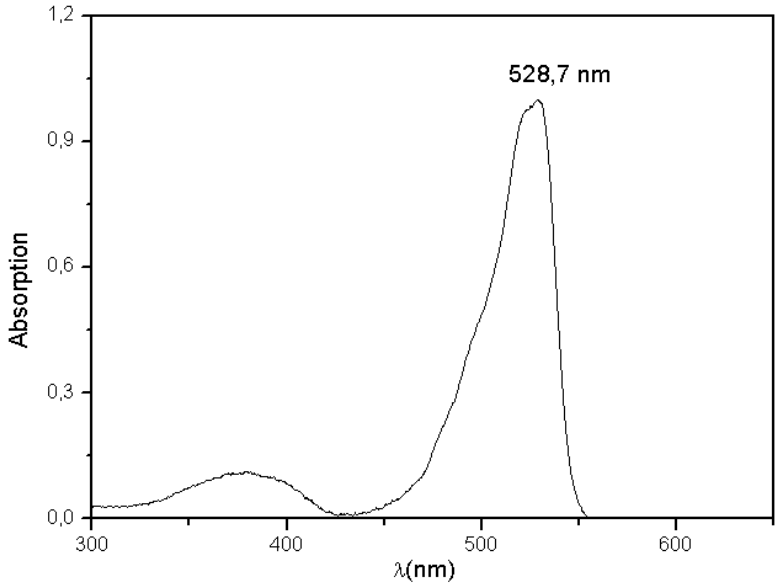

Figure 51- Absorption spectrum of Meso-Methyl-BODIPY.

In figure 52, in addition to the signs corresponding to the solvents, water at 1.56 ppm and hexane at 0.8 and 1.3 ppm[47], are also presented the peaks of protons of the BODIPY in protonic NMR. A triplet and a quadruplet correspond to the ethyl group. The other peaks, the three singlets correspond to the methyl groups.

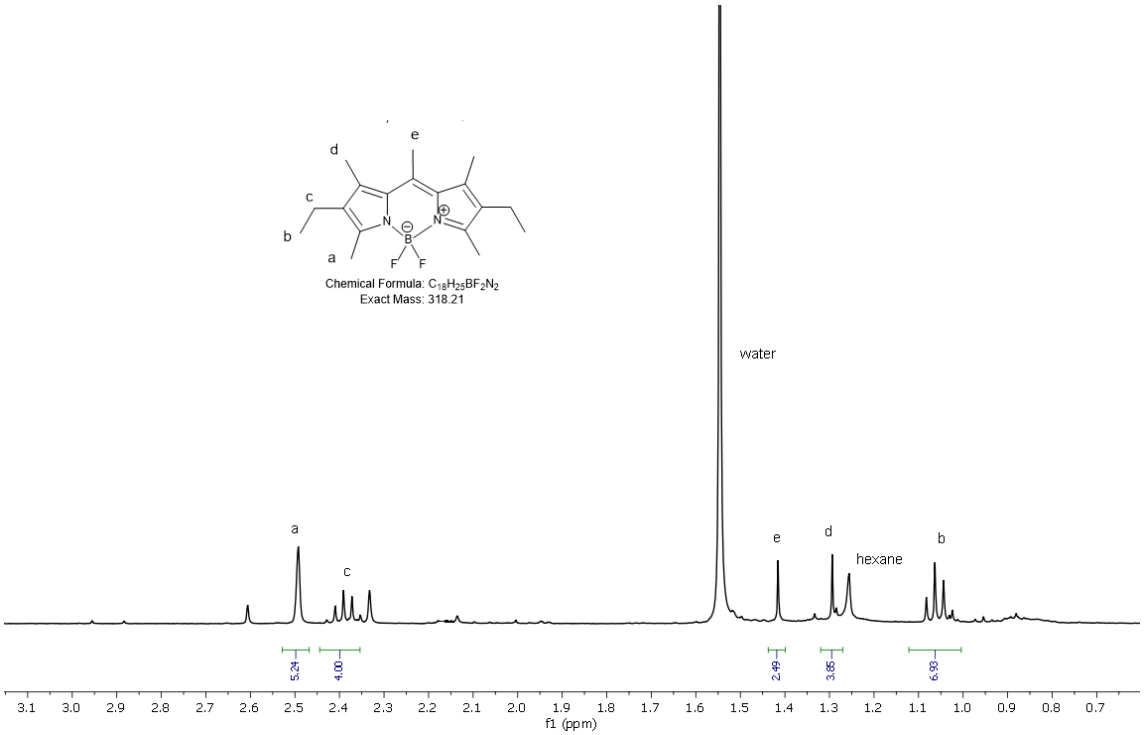

Figure 52- ^{1}H NMR spectrum of Meso-Methyl-BODIPY.

^{1}H NMR (400 MHz, $CDCl_3$) δ (ppm): 2.49 (s, 6H), 2.38 (q, J = 7.6 Hz, 4H), 2.17 (s, 3H), 1.29 (s, 6H), 1.06 (t, J = 7.6 Hz, 6H)

The mass spectrum presented in figure 53 is not a very good quality in terms of purity, and this may be due to low concentration. The spectrum shows the core at 305.3 m/z, which corresponds to the fragmentation resulting from the loss of the methyl group.

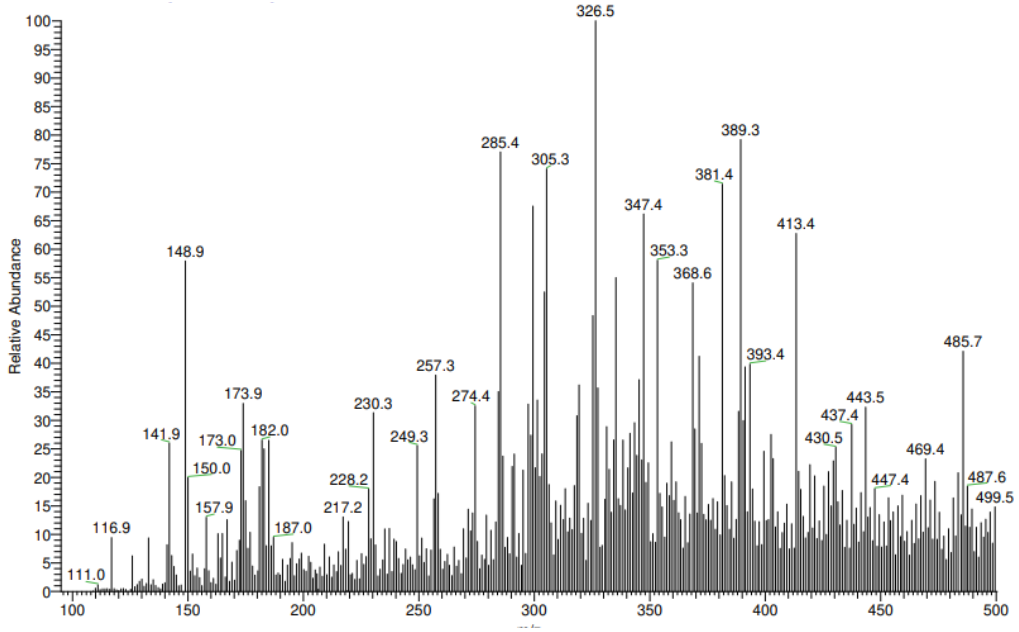

Figure 53- MS spectrum of Meso-Methyl-BODIPY.

The MS^2 spectrum shows the exact mass of the compound at 319.3 m/z and the fragmentations after the loss of fluorine, ethyl, and methyl groups (figure 54).

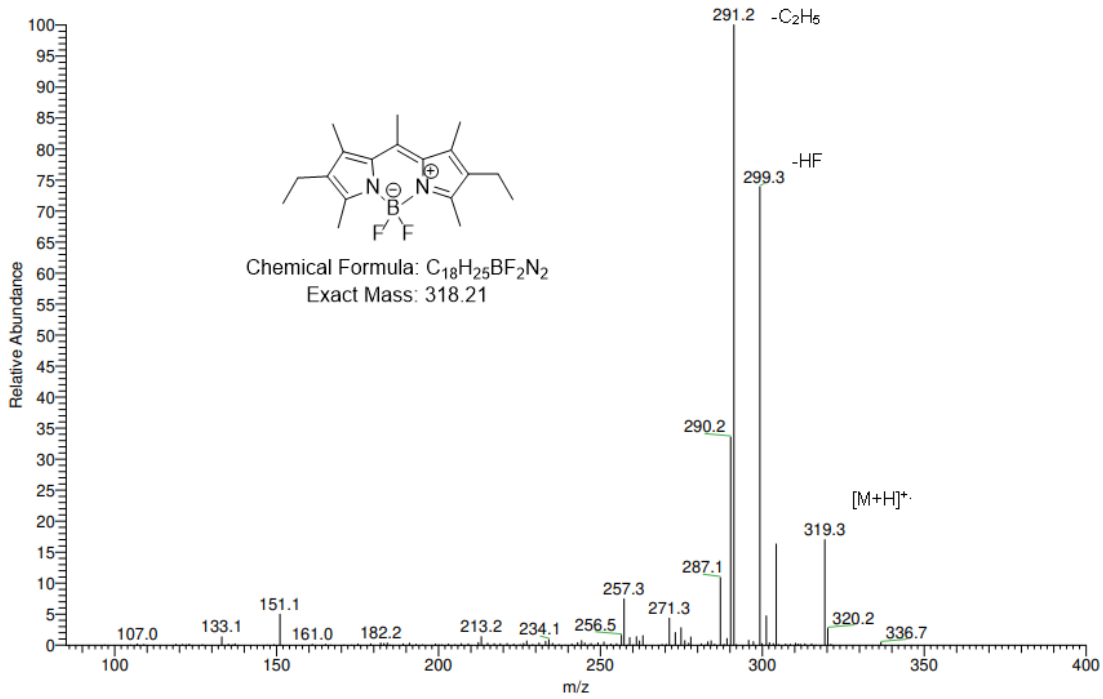

Figure 54- MS^2 of the Meso-Methyl-BODIPY.

3.3 Biological studies

After the synthesis and characterization of BODIPYs, the next step was to evaluate their potential as photosensitizers. The BODIPY dimer and Meso-Phenyl BODIPY were tested in two lung cell lines, A549 and H1299 (figure 55). The A549 is an adenocarcinoma human alveolar basal epithelial cells line, and the H1299 is a human non-small cell lung carcinoma cell line, derived from the lymph node.

(A) (B)

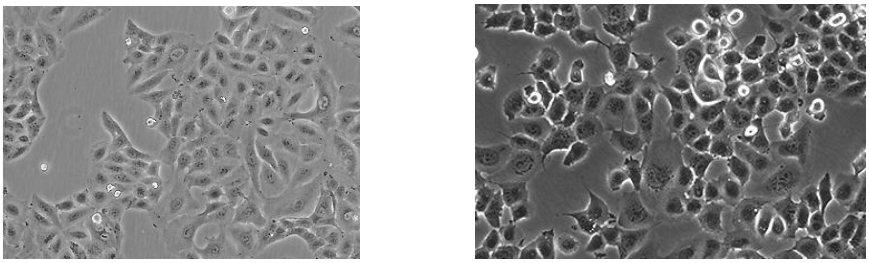

Figure 55- (A) A549 cell line (B) H1299 cell line.

The MTT assay was used to evaluate the cytotoxicity and phototoxicity of BODIPYs at different concentrations on the metabolic activity in A549 and H1299 cell lines, after 24 and 48 hours of incubation.

3.3.1 Metabolic activity

The first results presented in the figure 56 refer to the A549 cell line, The cytotoxicity of two BODIPYs was evaluated after 24 and 48 hours of incubation, and phototoxicity was measured for the same time after PDT.

For the A549 cell line, the BODIPY dimer did not show a cytotoxic effect for both times, nor with the increasing concentration. The cells which were submitted to PDT with light exposure until 10 J also maintained high values of metabolic activity. There were no significant differences between the two procedures, leading to the conclusion that BODIPY dimer is not a good photosensitizer for this cell line.

The Meso-Phenyl BODIPY showed to be cytotoxic for 24 and 48 hours when concentration increases. In terms of phototoxicity, metabolic activity decreases after PDT, with the differences being most noticeable for lower concentrations (≤ 10μM) in both times.

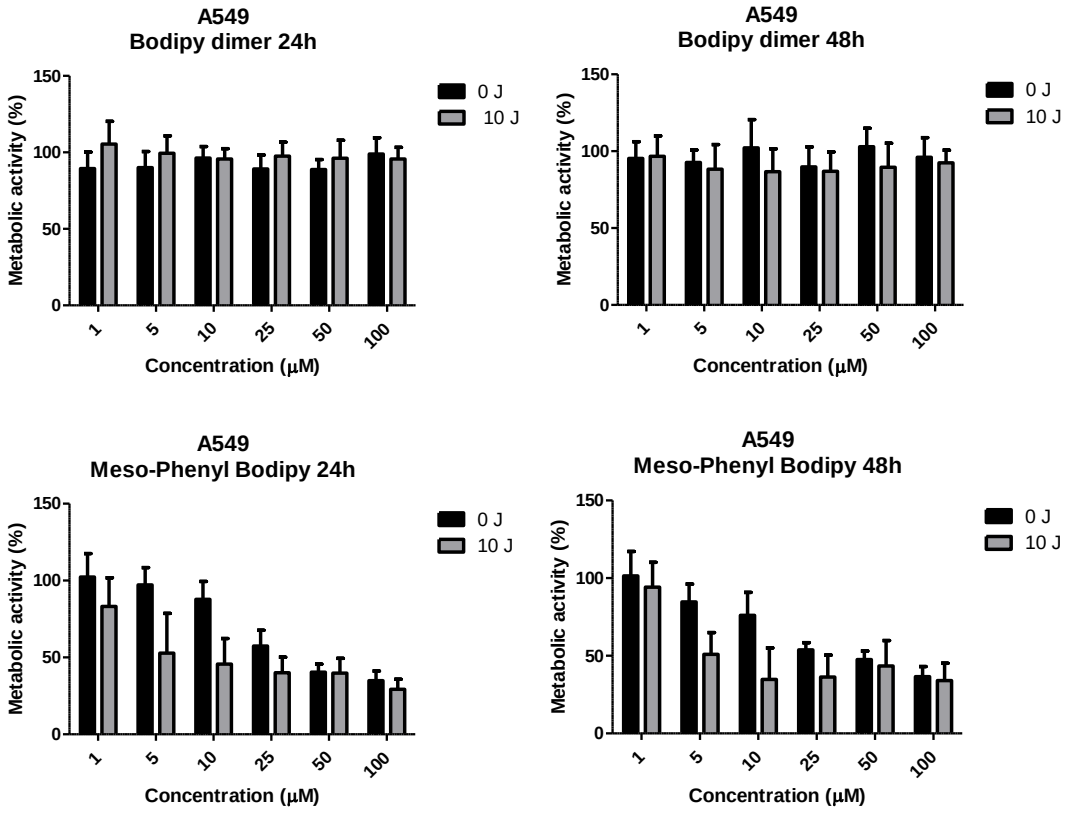

Figure 56 - Metabolic activity of BODIPY dimer and Meso-Phenyl BODIPY in the adenocarcinoma human alveolar basal epithelial cells, A549. Cells were incubated with

BODIPYs and maintained in the dark or submitted to PDT with light exposure until 10J. The evaluation of the metabolic activity was carried out after 24 and 48 hours. Results are presented as the mean and standard deviation of, at least, three experiments.

The next figure 57 showed the cytotoxic and phototoxicity of BODIPYs in the H1299 cell line. The BODIPY dimer revealed similar results to A549 cells. The cells presented high values of metabolic activity, once again the compound is not a good compound for application in photodynamic therapy.

The Meso-Phenyl BODIPY showed to be cytotoxic with a decrease in concentration at both times. The compound showed some phototoxicity for higher concentrations, mainly concentrations ≥ 25μM. These results are most noticeable 24 hours after PDT.

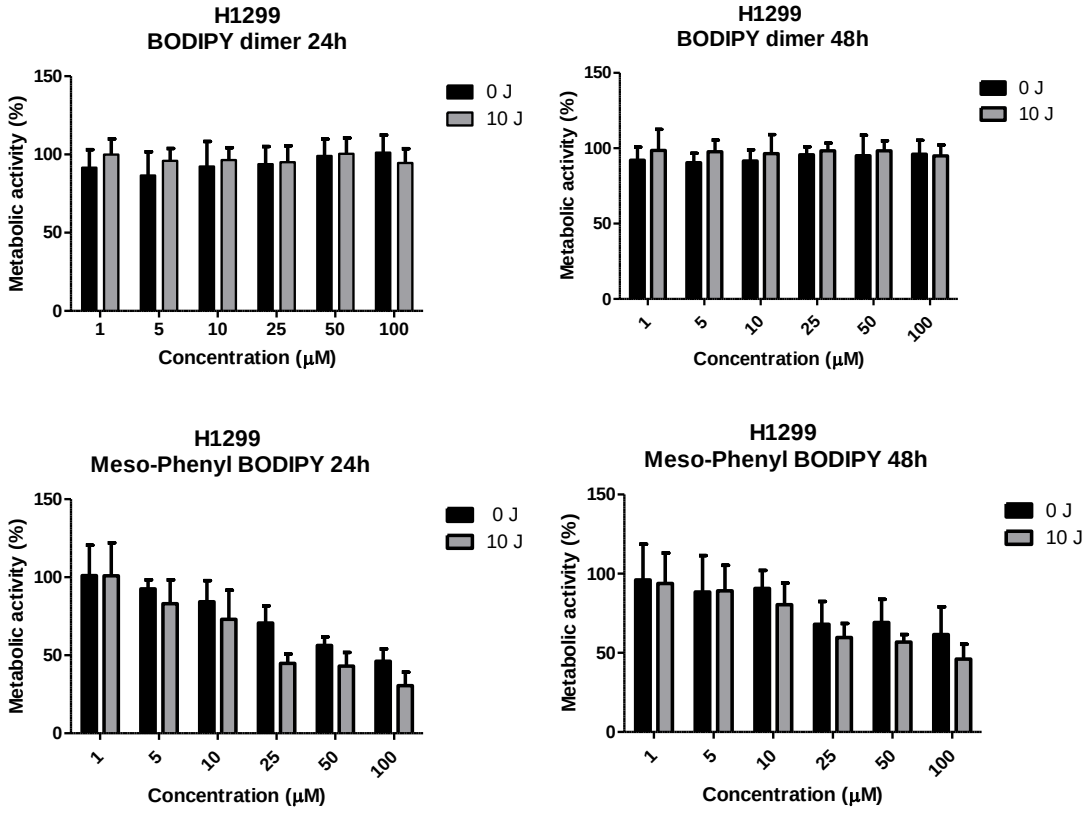

Figure 57 - Metabolic activity of BODIPY dimer and Meso-Phenyl BODIPY in the human non-small cell lung carcinoma cell line, H1299. Cells were incubated with BODIPYs and maintained in the dark or submitted to PDT with light exposure until 10J. The evaluation of the metabolic activity was carried out after 24 and 48 hours. Results are presented as the mean and standard deviation of, at least, three experiments.

From the two BODIPYs, Meso-Phenyl BODIPY was the one that showed some cytotoxicity and phototoxicity effect against both cell lines. However, the results are not as promising as some photosensitizers described in the literature. On the other hand, the BODIPY dimer has no effect as a photosensitizer in PDT. Since the compound shows no toxic effect on cells, it would be interesting to study this compound as a potential diagnostic molecule.

Chapter 4

Conclusions

The main objective of this research was to synthesize new BODIPYs. and evaluate their potential as photosensitizers in photodynamic therapy.

The BODIPY dimer had a very accessible synthesis, especially using THF. The product was pure and had a higher yield compared to the usual synthesis, using DCM as solvent. The fact that the formation of a by-product is not observed makes the purification process easiest. For this reason, the remaining BODIPYs were synthesized in THF.

Comparing the quantum yield of fluorescence of BODIPY dimer and Meso-Phenyl BODIPY, the first showed a higher value.

Another interesting synthesis in this work was the aliphatic BODIPYs. These BODIPYs are simple compounds that have identical reactional mechanisms to the aromatic ones.

They present small yields but are possible to purify. More synthesis and characterization are needed for aliphatic BODIPYs.

Biological studies were carried out for BODIPY dimer and Meso-Phenyl BODIPY. Metabolic activity was evaluated for two lung cell lines. The cytotoxicity and phototoxicity of the two BODIPYs was evaluated to find out their potential as photosensitizers. The Meso-Phenyl BODIPY showed some cytotoxicity and phototoxicity for both cell lines at higher concentrations. As the BODIPY dimer has no cytotoxicity and phototoxicity effect, could be studied as a molecule for photo-diagnosis.

Future perspectives

In terms of work in chemistry, a further study of aliphatic BODIPYs is needed to optimize the reaction and improve the yields. The low yields do not allow a complete characterization of the products.

As future work in biological studies, BODIPY trimer and aliphatic BODIPYs would start *in vitro* studies, evaluating their ability as photosensitizers.

More studies involving the BODIPY dimer and Meso-Phenyl BODIPY should be performed, such as SRB assay, and cellular uptake, the last to quantify the amount of BODIPYs which is inside the cell.

It would be interesting to find out whether a particular product, in this case, BODIPY dimer, had no effect on the cell because it may be biocompatible or whether it was unable to enter the cell and therefore had no effect. If the BODIPY dimer reveals to be biocompatible, it would be important to proceed to studies that evaluate its potential in diagnosis, due to its non-toxicity.

The sub-product of the trimer having a -COOH group will also be studied, since the -COOH group can allow for a better water solubility and cell uptake.

We intend to complete the characterization and biostudies and publish these results in an international journal.

References

1. Nicolaou KC. Organic synthesis: the art and science of replicating the molecules of living nature and creating others like them in the laboratory. *Proceedings Math Phys Eng Sci*. 2014;470(2163):20130690. doi:10.1098/rspa.2013.0690

2. Wall W, Pamulapati LG, Koenig RA, Dukat M, Caldas LM. Medicinal chemistry: The key to critical thinking in pharmacotherapy. *Curr Pharm Teach Learn*. 2022;14(3):253-257. doi:https://doi.org/10.1016/j.cptl.2022.01.003

3. Barker A, Kettle JG, Nowak T, Pease JE. Expanding medicinal chemistry space. *Drug Discov Today*. 2013;18(5):298-304. doi:https://doi.org/10.1016/j.drudis.2012.10.008

4. Andrew Davis; Simon E Ward. Handbook of Medicinal Chemistry: Principles and Practice. *R Soc Chem*. 2015. doi:10.1039/9781782621836

5. Zeki AA, Oldham J, Wilson M, et al. Statin use and asthma control in patients with severe asthma. BMJ Open, 2013:1-4. doi:10.1136/bmjopen-2013-003314

6. Giavina-bianchi P, Agondi R, Stelmach R, Cukier A, Kalil J. Fluticasone furoate nasal spray in the treatment of allergic rhinitis. Therapeutics and Clinical Risk Management 2008;4(2):465-472. doi: 10.2147/tcrm.s1984

7. Jung JA, Kim T, Kim J, et al. The Pharmacokinetics and Safety of a Fixed-Dose Combination of Acetylsalicylic Acid and Clopidogrel Compared With the Concurrent Administration of Acetylsalicylic Acid and Clopidogrel in Healthy Subjects : Single-Dose Crossover Study. *Clin Ther*. 2013;35(7):985-994. doi:10.1016/j.clinthera.2013.05.015

8. Papamichael K, Lin S, Moore M, Papaioannou G, Sattler L, Cheifetz AS. Infliximab in inflammatory bowel disease. 2019. 1-15 doi:10.1177/2040622319838443

9. Bunn HF, Katsumura KR, Devilbiss AW, et al. H. Franklin Bunn Cold Spring Harb Perspect Med 2013; doi: 10.1101/cshperspect.a011619

10. Hirose T, Kyu CC, Ahn J. Use of Insulin Glargine 100 U / mL for the Treatment of Type 2 Diabetes Mellitus in East Asians : A Review. 2019. doi:10.1007/s13300-019-0613-7

11. Seng H, Tiekink ERT, Lumpur K. *Main-Group Medicinal Chemistry Including Li and Bi* *. Elsevier Ltd.; 2013. doi:10.1016/B978-0-08-097774-4.00338-7

12. Kunimoto R, Bajorath J, Aoki K. From traditional to data-driven medicinal chemistry: A case study. *Drug Discov Today*. 2022;27(8):2065-2070. doi:https://doi.org/10.1016/j.drudis.2022.04.017

13. Roughley SD, Jordan AM. The Medicinal Chemist ' s Toolbox : An Analysis of Reactions Used in the Pursuit of Drug Candidates †. 2011.

14. Ding D, Xu S, da Silva-Júnior EF, Liu X, Zhan P. Medicinal chemistry insights into antiviral peptidomimetics. *Drug Discov Today*. 2023;28(3):103468. doi:https://doi.org/10.1016/j.drudis.2022.103468

15. Rivera G, Patel NB, Bandyopadhyay D. Editorial: Discovery and Development of Drugs for Neglected Diseases: Chagas Disease, Human African Trypanosomiasis, and Leishmaniasis . *Front Chem* . 2021;9.

https://www.frontiersin.org/article/10.3389/fchem.2021.775327.

16. Richman DD, Nathanson N. Antiviral Therapy. Third Edition. Elsevier (2016). Antiviral Therapy. Viral Pathogenesis, 271–287.doi:10.1016/B978-0-12-800964-2.00020-3

17. Malone B, Urakova N, Snijder EJ, Campbell EA. Structures and functions of coronavirus replication–transcription complexes and their relevance for SARS-CoV-2 drug design. *Nat Rev Mol Cell Biol*. 2022;23(1):21-39. doi:10.1038/s41580-021-00432-z

18. da Silva-Júnior EF. The 2022 Monkeypox outbreak: How the medicinal chemistry could help us? *Bioorg Med Chem*. 2022;73:117036. doi:https://doi.org/10.1016/j.bmc.2022.117036

19. Ferlay J., Ervik M., Lam F., Colombet M., Mery L. PM. Global Cancer Observatory: Cancer Today. Global Cancer Observatory: Cancer Today. International Agency for Research on Cancer; Lyon, France. https://gco.iarc.fr/today. Published 2018. Accessed May 24, 2022.

20. Rumgay H, Arnold M, Ferlay J, et al. Global burden of primary liver cancer in 2020 and predictions to 2040. *J Hepatol*. 2022;77(6):1598-1606. doi:10.1016/j.jhep.2022.08.021

21. Algorri JF, Ochoa M, Roldán-Varona P, Rodríguez-Cobo L, López-Higuera JM. Photodynamic Therapy: A Compendium of Latest Reviews. *Cancers (Basel)*. 2021;13(17):4447. doi:10.3390/cancers13174447

22. Hamblin MR. Special Issue Invited Review Photodynamic Therapy for Cancer : What ' s Past is Prologue . 2020:506-516. doi:10.1111/php.13190

23. Ackroyd R, Kelty C, Brown N, et al. The History of Photodetection and Photodynamic Therapy The History of Photodetection and Photodynamic Therapy. 2001; Photochemistry and Photobiology, 74(5), 656–669. doi:10.1562/0031-8655(2001)074<0656:THOPAP>2.0.CO;2

24. Von Tappeiner H. The History of Photodynamic Treatment. Munch Med Wochenschr. 1903;1:2042-2044. doi:10.1055/s−2005−861104

25. von Tappeiner H, Jodlbauer A. *Die Sensibilisierende Wirkung Fluorescierender Substanzen: Gesammelte Untersuchungen Über Die Photodynamische Erscheinung*. Vogel; 1907.

26. Diamond I, Mcdonagh A, Wilson C, Granelli S, Nielsen S, Jaenicke R. PHOTODYNAMIC THERAPY OF MALIGNANT TUMOURS. *Lancet*. 1972;300(7788):1175-1177. doi:https://doi.org/10.1016/S0140-6736(72)92596-2

27. Dougherty TJ, Grindey GB, Fiel R, Weishaupt KR, Boyle DG. Photoradiation therapy. II. Cure of animal tumors with hematoporphyrin and light. *J Natl cancer Inst*. 1975;55(1):115-121. doi: 10.1093/jnci/55.1.115

28. Kelly JF, Snell ME. Hematoporphyrin derivative: a possible aid in the diagnosis and therapy of carcinoma of the bladder. *J Urol*. 1976;115(2):150-151. doi: 10.1016/s0022-5347(17)59108-9

29. Dougherty TJ, Kaufman JE, Goldfarb A, Weishaupt KR, Boyle D, Mittleman A. Photoradiation therapy for the treatment of malignant tumors. *Cancer Res*. 1978;38(8):2628-2635. doi: 10.1007/978-94-009-0507-8_25

30. Dai T, Fuchs BB, Coleman JJ, et al. Concepts and principles of photodynamic therapy as an alternative antifungal discovery platform. *Front Microbiol*. 2012;3:120. doi:10.3389/fmicb.2012.00120

31. Baptista S, Cadet J, Mascio P Di, et al. Type I and II Photosensitized Oxidation Reactions: Guidelines and Mechanistic Pathways. 2016. doi:10.1111/ijlh.12426

32. Costa LD, Silva JDA, Fonseca SM, Arranja CT, Urbano AM, Sobral AJFN. Potential Sensitizer for Photodynamic Therapy. 21(4), 439 doi:10.3390/molecules21040439

33. Teixo R, Laranjo M, Serra A, et al. *740: Can Photodynamic Therapy Make a Difference in Retinoblastoma*? In Vivo Studies. Vol 50; 2014, European Journal of Cancer, 50, S177. doi:10.1016/S0959-8049(14)50649-1

34. Nascimento BFO, Laranjo M, Pereira NAM, et al. Ring-Fused Diphenylchlorins as Potent Photosensitizers for Photodynamic Therapy Applications: In Vitro Tumor Cell Biology and in Vivo Chick Embryo Chorioallantoic Membrane Studies. *ACS Omega*. 2019;4(17):17244-17250. doi:10.1021/acsomega.9b01865

35. Saini R, Lee N V, Liu KYP, Poh CF. Prospects in the Application of Photodynamic Therapy in Oral Cancer and Premalignant Lesions. 2016:1-14. European Journal of Cancer doi:10.3390/cancers8090083

36. Andersson-engels S. System for interstitial photodynamic therapy with online dosimetry : first clinical experiences of prostate. 2013. doi:10.1117/1.3495720

37. Loudet A, Burgess K. BODIPY Dyes and Their Derivatives: Syntheses and Spectroscopic Properties. *Chem Rev*. 2007;107(11):4891-4932. doi:10.1021/cr078381n

38. Ziessel R, Harriman A. The chemistry of Bodipy : A new El Dorado for fluorescence tools w. New journal of Chemistry, 2007:496-501. doi:10.1039/b617972j

39. Ulrich G, Ziessel R, Harriman A. The chemistry of fluorescent bodipy dyes: versatility unsurpassed. *Angew Chem Int Ed Engl*. 2008;47(7):1184-1201. doi:10.1002/anie.200702070

40. Zou B, Liu H, Mack J, et al. A new aza-BODIPY based NIR region colorimetric and fluorescent chemodosimeter for fluoride. *RSC Adv*. 2014;4(96):53864-53869. doi:10.1039/C4RA06416J

41. Verbelen B, Dehaen W. Postfunctionalization of the BODIPY Core : Synthesis and Spectroscopy, European journal of Organic Chemistry, 2015: 6577-6595. doi:10.1002/ejoc.201500682

42. Clarke RG, Hall MJ. *Recent Developments in the Synthesis of the BODIPY Dyes*. 1st ed. Elsevier Inc.; 2019. doi:10.1016/bs.aihch.2018.12.001

43. Zhao J, Xu K, Yang W, Wang Z, Zhong F. Chem Soc Rev modulation and application. *Chem Soc Rev*. 2015.44(24), 8904-8939 doi:10.1039/C5CS00364D

44. Kamkaew A, Lim SH, Lee HB, Kiew LV, Chung LY, Burgess K. BODIPY dyes in photodynamic therapy. *Chem Soc Rev*. 2013;42(1):77-88. doi:10.1039/C2CS35216H

45. Arranja T, Justino LLG, Castro RAE, et al. Double-tailed long chain BODIPYs - Synthesis , characterization and preliminary studies on their use as lipid fl uorescence probes, Journal of Molecular Structure 2017;1146:62-69. doi:10.1016/j.molstruc.2017.05.119

46. Encarnação T, Arranja CT, Cova TFGG, Pais AACC, Campos MG. Monitoring oil production for biobased feedstock in the microalga Nannochloropsis sp .: a novel method combining the BODIPY BD-C12 fluorescent probe and simple image processing. 2018;1. Journal of applied phycology, Volume 30, 2273-2285

47. Aguiar A, Farinhas J, Emilia M, Brett CMA, Morgado J, Sobral AJFN. Dyes and Pigments Synthesis , characterization and application of meso -substituted fl uorinated boron dipyrromethenes (BODIPYs) with di ff erent styryl groups in organic photovoltaic cells. *Dye Pigment*. 2019;168:103-110. doi:10.1016/j.dyepig.2019.04.031

48. Tram K, Yan H, Jenkins HA, Vassiliev S, Bruce D. The synthesis and crystal structure of unsubstituted 4,4-difluoro-4-bora-3a,4a-diaza-s-indacene (BODIPY). *Dye Pigment*. 2009;82(3):392-395. doi:https://doi.org/10.1016/j.dyepig.2009.03.001

49. Zhang W, Ahmed A, Cong H, Wang S, Shen Y, Yu B. Application of multifunctional BODIPY in photodynamic therapy. *Dye Pigment*. 2021;185:108937. doi:https://doi.org/10.1016/j.dyepig.2020.108937